

# OFDMA Schemes with Diversity in Frequency-Selective Fading Channels

*Ying Lin Xu*



Department of Electrical & Computer Engineering  
McGill University  
Montreal, Canada

July 2004

---

A thesis submitted to the department of Electrical and Computer Engineering and the committee on Graduate Studies in partial fulfillment of the requirements for the degree of Master in Engineering.

© 2004 Ying Lin Xu



Library and  
Archives Canada

Bibliothèque et  
Archives Canada

Published Heritage  
Branch

Direction du  
Patrimoine de l'édition

395 Wellington Street  
Ottawa ON K1A 0N4  
Canada

395, rue Wellington  
Ottawa ON K1A 0N4  
Canada

*Your file    Votre référence*

*ISBN: 0-494-06594-X*

*Our file    Notre référence*

*ISBN: 0-494-06594-X*

#### NOTICE:

The author has granted a non-exclusive license allowing Library and Archives Canada to reproduce, publish, archive, preserve, conserve, communicate to the public by telecommunication or on the Internet, loan, distribute and sell theses worldwide, for commercial or non-commercial purposes, in microform, paper, electronic and/or any other formats.

The author retains copyright ownership and moral rights in this thesis. Neither the thesis nor substantial extracts from it may be printed or otherwise reproduced without the author's permission.

#### AVIS:

L'auteur a accordé une licence non exclusive permettant à la Bibliothèque et Archives Canada de reproduire, publier, archiver, sauvegarder, conserver, transmettre au public par télécommunication ou par l'Internet, prêter, distribuer et vendre des thèses partout dans le monde, à des fins commerciales ou autres, sur support microforme, papier, électronique et/ou autres formats.

L'auteur conserve la propriété du droit d'auteur et des droits moraux qui protègent cette thèse. Ni la thèse ni des extraits substantiels de celle-ci ne doivent être imprimés ou autrement reproduits sans son autorisation.

---

In compliance with the Canadian Privacy Act some supporting forms may have been removed from this thesis.

Conformément à la loi canadienne sur la protection de la vie privée, quelques formulaires secondaires ont été enlevés de cette thèse.

While these forms may be included in the document page count, their removal does not represent any loss of content from the thesis.

Bien que ces formulaires aient inclus dans la pagination, il n'y aura aucun contenu manquant.

  
**Canada**

---

## Abstract

By using sufficiently long prefix and orthogonal narrow-band sub-carriers with adaptive bit loading, orthogonal frequency-division multiple-access (OFDMA) can offer high bandwidth efficiency required for broadband wireless access communications in frequency-selective fading channels. However, when deep fading occurs in a frequency slot, it can create data loss in one or more sub-carriers. Diversity techniques could be used to enhance the performance of OFDMA in the presence of deep fades.

The research presented in this thesis aims to provide diversity in OFDMA for broadband wireless access communications in frequency-selective fading channels. First, the diversity characteristics in OFDMA are examined to establish the diversity equivalence in the time and frequency domains. Based on these characteristics, suitable techniques to achieve the full diversity gain in OFDMA are developed. When channel information is available to transmitters, a group-optimal adaptive-tone-diversity OFDMA (GO-ATD-OFDMA) scheme that combines adaptive diversity gain and bit loading, is proposed. It is shown that the GO-ATD-OFDMA can offer a better performance than the conventional time-domain Rake receiver. In the case of unavailable channel information, spreading is combined with diversity in the proposed group-spreading OFDMA (GS-OFDMA) scheme to provide both diversity protection and interference suppression. The GS-OFDMA has a comparable performance to the group-orthogonal multi-carrier code-division multiple-access (GO-MC-CDMA) scheme but with a reduced transmitted peak-to-average power ratio (PAR). Performance of the proposed schemes in terms of error rates, spectral efficiency, achievable system throughput, and computational complexity is investigated by analysis and simulations.

## Sommaire

En utilisant un préfixe suffisamment long et des porteuses orthogonales à bande étroite en combinaison avec une allocation binaire adaptative, le multiplexage à accès multiple par répartition orthogonale de fréquences (OFDMA) peut offrir une grande efficacité spectrale requise pour les télécommunications sans-fil à très large bande sur canaux à évanouissements progressifs en fréquence. Par contre, l'évanouissement profond pour un certain intervalle de fréquence peut entraîner des pertes de données pour une ou plusieurs porteuses. Dans ce cas, différentes techniques de diversité pourraient être utilisées pour améliorer les performances OFDMA.

La recherche présentée dans ce mémoire a pour but d'offrir de la diversité pour la technique OFDMA pour les télécommunications sans-fil à très large bande sur canaux à évanouissements progressifs en fréquence. En premier lieu, les caractéristiques de la diversité pour la technique OFDMA sont étudiées afin d'établir l'équivalence entre la diversité dans les domaines temporels et fréquentiels. Basées sur ces caractéristiques, des techniques appropriées sont développées pour atteindre un gain de diversité complet pour l'OFDMA. Lorsque l'information du canal est disponible aux différents transmetteurs, une méthode de diversité appelée group-optimal adaptive-tone-diversity OFDMA (GO-ATD-OFDMA), qui combine un gain de diversité adaptatif avec un chargement de bit adaptatif, est proposée. Des recherches ont démontré que la méthode GO-ATD-OFDMA peut offrir de meilleure performance que le récepteur conventionnel de type rake. Dans le cas où l'information du canal n'est pas disponible, une méthode d'étalement est combinée avec une méthode appelée group-spreading OFDMA (GS-OFDMA) afin d'obtenir une protection sur la diversité et l'antiparasitage. La méthode GS-OFDMA a des performances comparables à la méthode groupe-orthogonal de multiple-accès de division de codes de multi-porteur (GO-MC-CDMA) avec l'avantage d'avoir un plus petit rapport de puissance de crête-à-moyen (PAR). Les performances de la méthode proposée

sont étudiées en fonctions du taux d'erreur, de l'efficacité spectrale, le débit possible du système et de la complexité informatique par l'entremise de simulation et d'analyse.

## Acknowledgments

First, I would like to express my deepest gratitude to my supervisor, Prof. Tho Le-Ngoc, for his valuable guidance and strong support during my graduate studies at McGill University. I would like to thank Dr. Jianfeng Weng for providing helpful suggestions and precious feedback to my research. I would also like to acknowledge NSERC for its financial support provided by the NSERC/eMPOWR Canada Innovation Platform Program.

I am thankful to my colleagues in Broadband Communications Lab for their encouragement and friendship. The constructive discussions with them are most appreciated. I am grateful to Frederic Monfet for the French translation of the abstract, and to Martino Freda for the proofreading of my thesis.

Finally, I am deeply indebted to my family. Without their love and support, this thesis would not have been possible.

# Table of Contents

<b>1</b>	<b>Introduction</b>	<b>1</b>
1.1	Multiple-Access in Multipath Fading Environments . . . . .	1
1.2	Thesis Objective and Contributions . . . . .	3
1.3	Thesis Outline . . . . .	4
<b>2</b>	<b>ZCZ-CDMA and OFDMA</b>	<b>6</b>
2.1	Multipath Fading Channels . . . . .	6
2.2	ZCZ-CDMA . . . . .	8
2.3	OFDMA as A Cyclic Non-Spreading CDMA Scheme . . . . .	10
2.4	Literature Reviews . . . . .	12
2.5	Chapter Summary . . . . .	15
<b>3</b>	<b>Diversity in OFDMA</b>	<b>16</b>
3.1	Assumptions, Structure and Signal Representations . . . . .	16
3.1.1	Research Assumptions and A General Structure . . . . .	16
3.1.2	Signal Representations . . . . .	18
3.2	Diversity Equivalence in Time- and Frequency-Domains . . . . .	21
3.2.1	Theorem on Diversity Equivalence . . . . .	21
3.2.2	Criteria on Selection of $L_f$ . . . . .	24
3.3	Tone-Combined Technique without Channel Information at Transmitters	25
3.3.1	TC-OFDMA . . . . .	25

3.3.2	BER Analysis . . . . .	27
3.4	Tone-Selective Technique with Channel Information at Transmitters . . .	29
3.4.1	TS-OFDMA . . . . .	29
3.4.2	BER Analysis . . . . .	31
3.5	Chapter Summary . . . . .	33
<b>4</b>	<b>Group-Optimal Adaptive-Tone-Diversity (GO-ATD) OFDMA for Transmitters with Channel Information</b>	<b>34</b>
4.1	Bit-Loading Technique with M-ary QAM . . . . .	35
4.2	Group-Optimal Adaptive-Tone-Diversity OFDMA . . . . .	39
4.3	System Performances . . . . .	41
4.3.1	System SER . . . . .	41
4.3.2	System Throughput . . . . .	42
4.3.3	Effects of Erroneous Channel Estimation . . . . .	43
4.4	Chapter Summary . . . . .	45
<b>5</b>	<b>Group-Spreading (GS) OFDMA for Transmitters without Channel Information</b>	<b>47</b>
5.1	GS-OFDMA System . . . . .	48
5.1.1	System Structure . . . . .	48
5.1.2	Reduced PAR . . . . .	51
5.1.3	Advantages and Disadvantage . . . . .	53
5.1.4	A Design Example . . . . .	53
5.2	Signal Model . . . . .	54
5.3	Optimal Multi-User Detection . . . . .	56
5.3.1	ML detector . . . . .	56
5.3.2	Effect of $N_s$ . . . . .	57
5.3.3	Performance of User-Loading Algorithm . . . . .	58



---

5.3.4	SER Performance Comparisons . . . . .	59
5.4	Chapter Summary . . . . .	61
<b>6</b>	<b>Conclusions</b>	<b>62</b>
6.1	Summary of Research Findings . . . . .	62
6.2	Suggestions for Future Research . . . . .	65
<b>A</b>	<b>BER Derivation of TS-OFDMA</b>	<b>67</b>
	<b>References</b>	<b>71</b>

# List of Figures

2.1	Multitpath transmission of wireless communications . . . . .	7
2.2	Despreading window for ZCZ sequence with prefix and suffix . . . . .	9
2.3	Block diagram of OFDMA transceiver . . . . .	11
3.1	Block diagram of an uplink OFDMA system. . . . .	17
3.2	Energy ratio for $L_f$ not divisible by $N$ . . . . .	23
3.3	The formation of sub-carrier group . . . . .	24
3.4	BER performance of TC-OFDMA with various M-ary QAM . . . . .	29
3.5	BER performance of TS-OFDMA with various M-ary QAM. . . . .	32
4.1	Actual SER with bit-loading technique. . . . .	42
4.2	Throughput comparison between GO-ATD-OFDMA and RH-OFDMA. . . . .	43
4.3	Throughput ratio $S_{GO-ATD}/S_{OPT}$ at different system load. . . . .	44
4.4	Degradation of SER for various error levels in channel estimation . . . . .	46
5.1	Sub-carrier and sub-stream assignment of GS-OFDMA . . . . .	50
5.2	Difference in input signals by sending two sequences . . . . .	51
5.3	SER comparison between GS-OFDMA and GO-MC-CDMA . . . . .	57
5.4	The effect of $N_s$ on the error rate performance . . . . .	58
5.5	SER performance of GS-OFDMA at different system load . . . . .	59
5.6	SER comparison of different multi-carrier systems . . . . .	60

# List of Tables

4.1	The threshold values for different modulation schemes . . . . .	38
4.2	SNR gaps required for different symbol error rates . . . . .	39
5.1	Reduced PAR for different $N_s$ . . . . .	52
5.2	Performance metrics comparisons of multi-carrier schemes . . . . .	53

# List of Symbols

$\mathcal{A}$	Amplitude of signal
$C$	Sub-carrier allocation function
$D$	Distance between two points in signal constellation
$E$	Energy of transmitted symbol
$E_b$	Energy of transmitted bit
$\mathcal{F}$	Matrix of multipath transformation
$H$	Fourier transform of $\beta$
$K$	Number of active users
$L_{CPI}$	Length of CPI
$L_f$	Number of sub-carriers occupied
$L_{k,t}$	Number of multipath before transformation
$L_t$	Number of taps of the transformed channel model
$M$	Order of QAM modulation
$N$	Number of sub-carriers (or spreading gain in CDMA)
$N_o$	Power spectrum density of noise
$N_p$	Number of samples in a symbol (with CPI)
$N_s$	Number of sub-streams from a user
$P$	Error probability
$R$	Cross-correlation matrix
$S$	Symbol in frequency domain

---

$T$	Period of sampling
$V$	Sample of received signal
$W$	Fourier transform of $\eta$
$Y$	Fourier transform of $V$
$a$	Chip of spreading sequence
$c$	Chip index
$d$	Symbol of sub-stream
$f_b$	Data rate
$f_c$	Chip rate
$i$	Sample index
$k$	User index
$l$	Path index
$m$	Sub-carrier index
$m_o$	First sub-carrier index in a group
$n$	Symbol interval index
$o$	Order of PAM modulation
$p$	Probability density function
$q$	Variable to decide the value of $k$
$s$	Transmitted time-domain signal
$t$	Time index
$u$	Sub-stream index
$\Gamma$	SNR gap
$\alpha$	Fading parameter before transformation
$\beta$	Fading parameter after transformation
$\gamma$	Signal-to-noise ratio
$\eta$	Gaussian random variable with mean of zero
$\tau$	Time delay of path

# Chapter 1

## Introduction

### 1.1 Multiple-Access in Multipath Fading Environments

Code-division multiple-access (CDMA) technique has attracted considerable attention due to its potentials of high spectral efficiency, asynchronous access, and good resistance against multipath fading. In a CDMA system, users' signals with data rate of  $f_b$  are first spread at a chip rate of  $f_c$  (much higher than  $f_b$ ) by their user-specific spreading sequences, and then transmitted simultaneously in the shared system frequency band. At the receiver, all the users' signals are received and a particular user signal of interest can be extracted by de-spreading the received signal with its corresponding user-specific spreading sequence. Because of the good cross-correlation property of the spreading sequences, the receiver can demodulate only the information carried by the known spreading sequence and treat other users' signals as multiple-access interference (MAI). When there is a sufficiently high processing gain (defined as the ratio of  $f_c$  over  $f_b$ ), the MAI can be suppressed. On the other hand, the good auto-correlation property of the spreading sequence also enables the receiver to combine the fading replicas in multiple fading channels, resulting in a time-domain diversity gain and an improved performance. The capabilities of CDMA has made it popular and widely used in personal communications

systems (PCS).

For broadband wireless access systems, as the required user data rate ( $f_b$ ) increases while the available system bandwidth is limited, the offered processing gain,  $f_c/f_b$ , has to be reduced and the interference suppression capability of CDMA is consequently limited.

This has recently created the growing interest in considering orthogonal-frequency-division multiple-access (OFDMA) [1, 2] for broadband multimedia wireless access systems.

In OFDMA, the system bandwidth is divided into a large number of orthogonal overlapping narrow-band sub-carriers that can be shared among the users. With a sufficiently narrow band, each sub-carrier only “sees” *flat* fading even though frequency-selective fading occurs over the entire system band. As such, the signal detection in each sub-carrier is much simpler and a spectrum-efficient quadrature amplitude modulation (QAM) scheme can be used. By inserting a cyclic prefix longer than the channel delay spread to maintain the orthogonality between sub-carriers [3], OFDMA offers good performance in frequency-selective fading channels. In addition, using bit loading adapted to available signal-to-noise ratios (SNR) in different sub-carriers can enhance both bandwidth and power efficiencies of the system.

However, deep fades can occur in the system band and create extremely low SNR in one or more sub-carriers, which results in data losses. Furthermore, in time-varying frequency-selective fading channels, both the occurrence and locations of deep fades are non-deterministic. Diversity techniques can be applied to OFDMA to improve its performance in the presence of random deep fades.

Two diversity techniques for OFDMA have been considered. One makes use of slow-hopping OFDMA to add diversity to a frame of symbols in conjunction with a powerful coding scheme [4, 5]. Erased symbols transmitted on sub-carriers suffering deep fades can be recovered by the decoder. The coding scheme in slow-hopping OFDMA may require low coding rate and iteration decoding procedures, and hence reduce the system

speed and bandwidth efficiency. The other technique uses more antennas at the base station to provide space diversity. Improvement in system performance is achieved at a cost of infrastructure.

## 1.2 Thesis Objective and Contributions

The research presented in this thesis aims to develop cost-effective techniques to incorporate diversity in OFDMA. It covers the following aspects:

- Investigation of diversity characteristics in OFDMA.
- Development of OFDMA schemes with diversity by exploring its diversity characteristics.

Both analysis and simulations have been carried out to evaluate the performance of the developed techniques.

The contributions of this thesis are listed below.

- The diversity equivalence between CDMA in time domain and OFDMA in frequency domain is analytically derived. It is shown that, similar to the Rake receiver for CDMA, full diversity gain can be obtained in OFDMA with a number of sub-carriers equal to the number of paths representing the multipath frequency-selective fading channel.
- Based on the above results, a systematic sub-carrier assignment method for OFDMA that achieves full diversity gain is proposed.
- A tone-selective (TS) technique for the case of channel information available at transmitters and a tone-combined (TC) technique for the case of no available channel information at transmitters, are developed based on the derived diversity characteristics to support a limited number of users. Their performance for



OFDMA with M-ary QAM signaling over multipath frequency-selective Rayleigh fading channels is analyzed.

- A group-optimal adaptive-tone-diversity (GO-ATD) OFDMA scheme is further developed for the case of channel information available at transmitters. The scheme achieves not only adaptive diversity gain in a frequency-selective fading environment, but also has negligible throughput degradation and low computational complexity compared to the system with the optimal sub-carrier assignment scheme.
- By combining spreading with the TC technique, a group-spreading (GS) OFDMA scheme is proposed for the case of no available channel information at transmitters. The GS-OFDMA provides diversity gain, and mitigates the effect of interference at the same time. The GS-OFDMA scheme has an error rate performance close to the single-user Rake receiver. In addition, with its split-and-group structure, it provides reduced peak-to-average power ratio (PAR) and needs relaxed channel estimation as compared to the group-orthogonal (GO) MC-CDMA scheme.

### 1.3 Thesis Outline

The rest of this thesis is organized as follows.

After a brief review of multipath frequency-selective fading in wireless channels, Chapter 2 examines the equivalence between zero-correlation-zone (ZCZ) CDMA and OFDMA. The perfect correlation property of ZCZ code in quasi-synchronized multipath fading environment, and its disadvantage of limited family size are explained. Sharing the similar idea of cyclic insertion in ZCZ sequences, OFDMA can be regarded as a special case of ZCZ-CDMA while having the advantage of a much larger family size. The transceiver structure, advantages and disadvantages of OFDMA are highlighted. A literature survey on diversity techniques is presented.

Chapter 3 mainly addresses the diversity characteristics of OFDMA. Diversity equivalence between time-domain and frequency-domain transmissions is examined. The minimum number of sub-carriers required to achieve the same diversity gain as in the time-domain Rake receiver is derived. Based on the frequency-diversity characteristic, the TC and the TS techniques with a systematic sub-carrier assignment scheme are proposed. Their performance is evaluated.

In Chapter 4, to improve the spectral efficiency of TS-OFDMA, a GO-ATD technique that combines adaptive sub-carrier selection diversity and bit loading is proposed when channel information is available at transmitters. Its performance and complexity are evaluated.

Chapter 5 describes the proposed group-spreading (GS) OFDMA scheme for the case of unavailable channel information. Its structure, PAR, advantages and disadvantages are discussed with a design example. Its performance with maximum-likelihood multiuser detection (MUD) is examined.

Chapter 6 provides concluding remarks and suggests some topics for further studies.

## Chapter 2

# ZCZ-CDMA and OFDMA

In this chapter, we first explain the multipath characteristic of wireless channels, and describe its effects on signal transmissions in Sec.2.1. Then the design of zero-correlation-zone (ZCZ) CDMA system is introduced in Sec.2.2 as a solution to achieve interference-free transmissions in a multipath fading environment. However, the drawback in the family size of the ZCZ code prevents its practical implementation. In Sec.2.3, OFDMA is examined as a non-spreading form of ZCZ-CDMA, but with a larger family size than that of the ZCZ code. Finally, literature reviews on current research trends to combat the multipath fading characteristic of wireless channels is given in Sec.2.4.

### 2.1 Multipath Fading Channels

The multipath fading in wireless transmissions is caused by three basic propagation mechanisms: reflection, diffraction, and scattering. As long as there is a surrounding environment, such as buildings, cars, trees, etc., the three mechanisms will generate multipath setting for signal propagation. Hence, the signals received will be a combination of signals that have gone through distinct paths. The combination could be constructive or destructive, resulting in the power fluctuation on the received signals. Fig.2.1 shows a scenario of 3 distinct signal propagation paths.

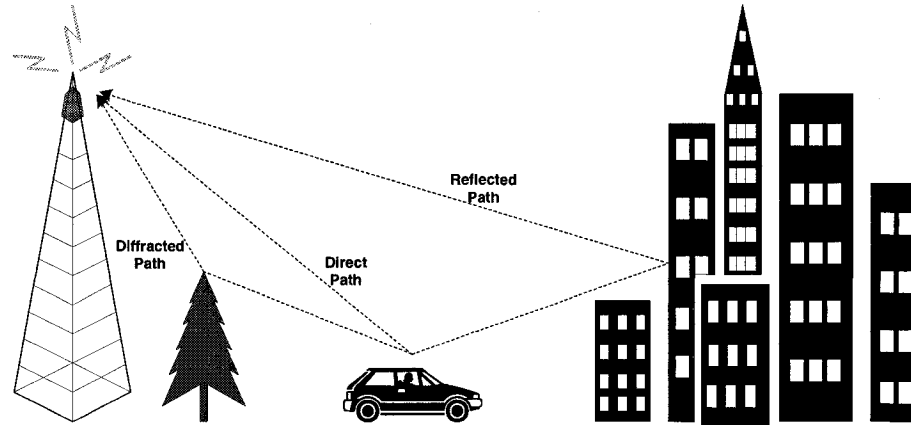


**Fig. 2.1** Multipath transmission of wireless communications

The multipath characteristic creates interference in an access environment. Interference is induced when signals from distinct paths collide. In CDMA systems, orthogonal sequences can be applied to separate users. However, the multipath characteristic of channels introduces several signal replicas with different delays. These replicas bear the same spreading sequence, and interfere with each other. The amount of interference depends on the auto-correlation property of the spreading sequence. Large amount of interference is generated if the shifted versions of the spreading sequence are highly correlated; while little interference is formed if they are almost orthogonal. On the other hand, the effect of interference also depends on the strengths of the replicas. Signals from weaker paths are corrupted due to the large interference from stronger paths, and hence combining those signals will not help on detection. Therefore, even with a Rake receiver, the performance improvement is limited. Moreover, signal replicas of other users also create MAI to the decoded signal due to the fact that the orthogonal sequences only have zero cross-correlations if they are undistorted and synchronous, and such conditions can be hardly satisfied when signals pass through different multipath channels in an uplink environment.

Fading is another impact brought by the multipath characteristic. After passing through multipath channels, signals might experience both large-scale and small-scale

fading. The large-scale fading describes the mean strength of received signals. The common models for the large-scale fading include the Longley-Rice model, the Durkin's model, the Okumura model, the Hata model, the Walfisch and Bertoni model as shown in Sec. 3.10 of [6]. While the small-scale fading predicts the short-term fluctuation of received signal strength. Rayleigh and Ricean distributions are frequently used to characterize the statistically varying nature of small-scale fading. Since the large-scale fading changes over a relatively long period of time, its effect usually can be compensated for by power controls [7, 8]. In this research, we assume an open-loop power control in uplink transmissions to eliminate the large-scale fading effect. However, the rapid varying characteristic of the small-scale fading makes it hard to compensate, so the small-scale fading has to be considered in the signal model. To combat small-scale fading, we have to employ diversity in the system. Diversity gain can be realized by either receivers or transmitters.

- Diversity gain by receivers can be obtained by collecting signal energies from all paths. However, to avoid contamination in multipath replicas, the orthogonality must be maintained among the multipath signals. This diversity method is known as maximum ratio combining (MRC).
- Diversity gain by transmitters can be achieved by sending the same signal over multiple carriers which have independent conditions. If channel conditions are known in advance, then the method of selection diversity (SD) which picks the best carrier for transmission seems appealing as it can avoid the waste of signal energy on bad carriers.

## 2.2 ZCZ-CDMA

For CDMA systems, to preserve the signal orthogonality over multipath fading channels, the idea of binary ZCZ code sequences is proposed [9, 10]. The design of the ZCZ

sequences is an extension of generating complementary sequences. The binary ZCZ code has perfect auto-correlation and cross-correlation properties, meaning the cross-correlation and out-of-phase auto-correlation are always zero if the timing shift is within the designed range. The detailed construction of ZCZ sequences can be found in [10].

If the length of the zone is larger than the longest delay of any of the users, the ability to maintain zero cross-correlation can help users to maintain orthogonality in a quasi-synchronous multipath CDMA system [11]. However, due to its special design, while even-cross-correlations<sup>1</sup> are always zeros, the ZCZ code cannot guarantee the odd-cross-correlations<sup>2</sup> are zeros. To overcome the odd-cross-correlation problem in quasi-synchronous environment, we can add a cyclic prefix and cyclic suffix to each information bit interval. For example, if the timing offset between signals can be controlled within  $[-0.5, 0.5]$  chip, Fig. 2.2 illustrates that one chip prefix and one chip suffix are required in order to maintain the orthogonality of each signal. The despreading window shown in

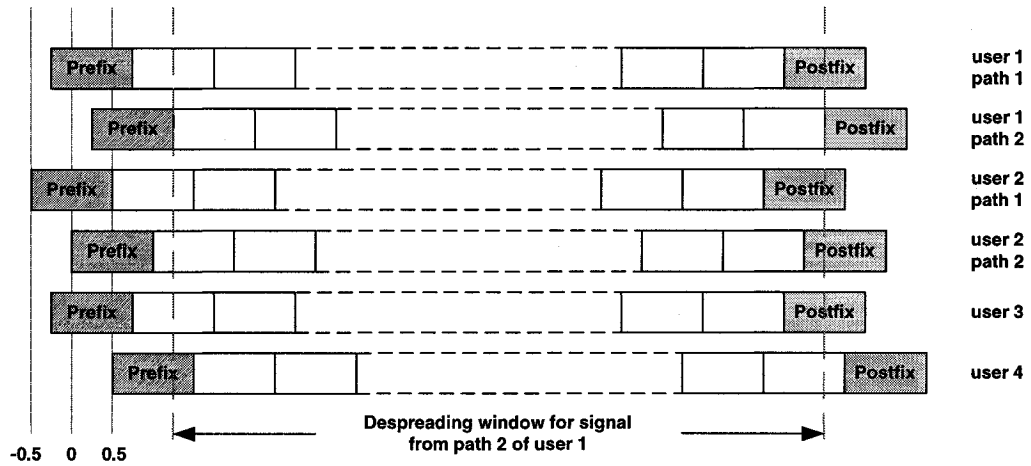


Fig. 2.2 Despreading window for ZCZ sequence with prefix and suffix

the figure is for the signal from path 2 of user 1. When despreading the received signal,

<sup>1</sup>Even-cross-correlation happens when all information bits unchanged during the period of one despreading window.

<sup>2</sup>Odd-cross-correlation occurs when any information bit is changed in the middle of one despreading window.

the cyclic prefix and the cyclic suffix of the signal of interest are chopped off, and only the chips left are used for despreading. A coherent receiver is assumed in this case so the receiver always knows the beginning of the despreading window. In such scenario, the Rake receiver is preferred in order to collect all the delayed versions of the same signal [12, 13].

ZCZ-CDMA can eliminate interference caused by both multiple-access and multipath fading. However, this achievement is accomplished at the cost of a reduced family size of the ZCZ code. With a given spreading gain of  $N$ , the maximum number of ZCZ sequences we can have for a zone with length of  $L_z$  is  $\lfloor N/L_z \rfloor$  [14]. As we can see, the family size of the code is inversely related to the zone length. As the zone length increases, the family size reduces further. Hence, the family size of the ZCZ code sequences might be too small to apply in practical systems.

### 2.3 OFDMA as A Cyclic Non-Spreading CDMA Scheme

The insertion of a cyclic prefix in the ZCZ-CDMA system reminds us of the OFDMA system. OFDMA also requires a cyclic prefix in order to maintain the orthogonality of users. Normally, a blank guard time with length longer than the largest delay induced by channels can get rid of the interference from the last symbol. So with empty guard time inserted, the received OFDM symbol is guaranteed to be free of inter-symbol-interference (ISI). However, with blank guard time, the orthogonality between users cannot be maintained. One intuitive explanation of this can be found in Sec. 2.3 of [15] by counting the numbers of cycles sine waves have in an observation window. Sine waves with different periods represent sub-carriers with different frequencies. For orthogonality, all sine waves must have complete cycles in the observation window so that their integration within the window always returns zero. With the blank guard time, the numbers of cycles will not be integers, and hence the orthogonality property between sub-carriers is

lost. To overcome this problem, each sub-carrier can be cyclically extended in the guard time. By filling the guard time with the cyclic information, the numbers of cycles in the observation window are ensured to be integers, and hence MAI is avoided.

The frequency separation of OFDMA is achieved by discrete Fourier transform (DFT). Fast Fourier transform (FFT), as an efficient implementation of DFT, can simplify the design of transmitter and receiver, and provide faster computation. Fig. 2.3 shows a transceiver structure of OFDMA. A general case with single user occupying sev-

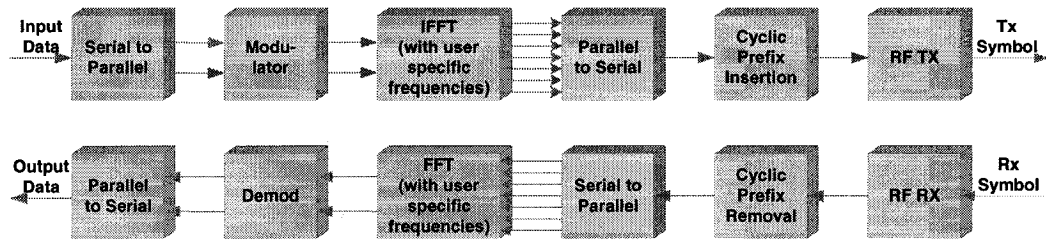


Fig. 2.3 Block diagram of OFDMA transceiver

eral sub-carriers is drawn in the figure. In the transmitter, a user's data is first converted to several parallel inputs, then the inputs are transported by the sub-carriers that is assigned to the user. The IFFT operation is performed on those sub-carriers to transform the frequency-domain signals to time-domain. As the time-domain signals can only be sent sequentially, the outputs of IFFT should be parallel-to-serial converted as shown in the figure. To prevent the loss of orthogonality of sub-carriers over fading channels, a cyclic prefix is inserted in the time-domain signal. At this point, the time-domain signal is ready to be amplified and transmitted over the medium. Reverse operations to the transmitter are carried out in the receiver. Generally speaking, the most important operations in the transceiver are FFT and IFFT.

If the multiplication of an exponential sequence (i.e., IFFT operation) in OFDMA is regarded the same as the multiplication of a spreading sequence in CDMA, OFDMA can be considered as a special form of CDMA [16]. In OFDMA, the signal spectrum is not spread and the cyclic prefix keeps all the interference away. Hence, OFDMA is a



special CDMA scheme with a non-spreading ZCZ code. Furthermore, the family size of the non-spreading ZCZ code used in OFDMA is not limited by the length of the zone.

Overall, the OFDMA scheme has several advantages.

- OFDMA has high spectral efficiency as DFT operation creates sub-carriers with overlapped sidebands but not mutual interference.
- OFDMA is an effective way to handle multipath propagation. As long as the cyclic prefix is longer than the largest delay, its transmission is free of multipath interference.
- If transmitters know channel information, the performance of OFDMA system can be improved by bit loading algorithm. This technique has been already applied to digital subscribe line (DSL) technology [17].
- OFDMA can be easily implemented by FFT/IFFT operation, which means the implementation cost is low.

Nevertheless, OFDMA also has its limitations as compared to ZCZ-CDMA. For example, its frequency-domain transmission lacks diversity protection. If multiple sub-carriers are used to add diversity, the problem of large PAR occurs. The PAR of OFDMA with  $L_f$  sub-carriers per user can be written as  $10 \log(L_f)$  in dB. As the number of sub-carries goes up for more diversity, the PAR also increases. Large PAR requires large input back-off at the power amplifier, otherwise clipping will destroy the orthogonality property between sub-carriers. Meanwhile, large input back-off of the power amplifier implies low power efficiency, and hence a waste of resource.

## 2.4 Literature Reviews

In a multipath frequency-selective fading environment, the issues of interference minimization and diversity gain have been addressed extensively by many papers in the

literature [18, 19, 20].

In order to suppress interference in CDMA, special code designs have been proposed for quasi-synchronous systems [21, 22, 9, 23, 10]. The preferentially-phased Gold (PP-Gold) code in [21] was proven to reduce the MAI if timing offset was within  $\pm 0.5T_c$ , where  $T_c$  was the chip interval. In [22], a class of sequences with small cross-correlation was designed for a more general case which had timing offset within few chip intervals. Furthermore, a set of polyphase sequences in [9] was introduced as a solution to bring zero cross-correlation in additive white Gaussian noise (AWGN) channels. However, the out-of-phase auto-correlations of the above three codes have non-zero values, and hence ISI cannot be avoided in a multipath fading environment. Then in [23], the idea of polyphase code was further extended to have zero out-of-phase auto-correlation and small cross-correlation properties in selective fading channels. Nevertheless, the design still cannot achieve interference-free transmission in multipath fading channels. Besides, its non-binary characteristic discourages its practical implementation. To remedy the problem, the design of ZCZ code was presented to achieve totally interference-free transmission in multipath frequency-selective fading channels. Nevertheless, as mentioned in Sec. 2.2, the family size of ZCZ sequences is sacrificed for the perfect correlation properties in the code design, which may raise concern in practical implementations.

On the other hand, to add diversity for symbol detection in OFDMA, one well-known solution is to transmit the same signal over multiple sub-carriers. The performance improvement provided by this frequency diversity method was promising [24]. The question then arises as to how frequency diversity should be designed without knowing the information of channels in advance, more specifically, how many sub-carriers are necessary and how we locate them. It is widely accepted that the more sub-carriers we use, the more diversity we gain, and hence less spectral efficiency we realize. To balance the trade-off between diversity gain and spectral efficiency, we refer to the maximum diversity that can be achieved by Rake receiver in the time domain as the full diversity

gain, then our question becomes how we can achieve the full diversity gain in frequency domain while keeping the system spectral efficiency as high as possible. To answer the second part of the question, we recall that spreading can help us efficiently utilize the spectrum. Therefore, the question becomes how to achieve full diversity for a general multi-carrier (MC) system that combines both OFDMA and spreading.

For a general MC system, it was [25] that first pointed out the relationship between channel order and the required number of sub-carriers for full diversity gain in a multipath fading channel. Developed from the relationship, a generalized MC-CDMA (GMC-CDMA) structure was presented to eliminate MAI and achieve full diversity gain [25]. Based on the same idea, a mutually-orthogonal usercode-receiver (AMOUR) structure was proposed for quasi-synchronous blind CDMA that eliminates MAI deterministically and mitigates frequency-selective fading regardless of the multipath and modulation [26]. The success of both structures relies on the block spreading which assumes that the channel conditions are time-invariant over the period of a transmitted block. Then in [27], a channel independent block spreading schemes was developed for double selective (time- and frequency-selective) channels. Nevertheless, while MAI is eliminated in the above proposals, existing ISI limits the system performances. This leads to the idea of a group-orthogonal (GO) MC-CDMA system [28], in which full diversity gain was reached and ISI was eliminated. While MAI existed among a small group of users, MUD was practically feasible to mitigate the effect of MAI. Unfortunately, by grouping sub-carriers, the issue of high PAR in multi-carrier transmissions arises in GO-MC-CDMA. This creates practical concern of power efficiency if a large number of sub-carriers is required to obtain the full diversity gain.

Even though much effort has been devoted to minimizing interference and improving diversity gain in a multiple access environment, current technologies for 3G systems and beyond still cannot solve the two issues practically, especially in uplink systems characterized by non line-of-sight (LOS), and multi-reflection transmissions.

## 2.5 Chapter Summary

In this chapter, we reviewed the multipath characteristic of wireless communications. In particular, to overcome the interference problem induced by the multipath fading characteristic, the scheme of ZCZ-CDMA has been proposed for a quasi-synchronous system. ZCZ-CDMA successfully removes all ISI and MAI, which simplifies the use of a Rake receiver. One disadvantage of the ZCZ code is its reduced family size. On the other hand, with cyclic prefix insertion, OFDMA can be regarded as a non-spreading ZCZ-CDMA. The equivalent code family size in OFDMA is the number of its FFT points, which is much larger than that in ZCZ-CDMA. Hence, OFDMA can provide interference-free transmissions to a large number of users over multipath frequency-selective channels. However, the frequency-selective characteristic in broadband systems requires diversity protection in the OFDMA scheme. As literature reviews show no practical solution exists yet to solve the problem, we are inspired to find a diversity technique in the aim of protecting the transmissions in OFDMA.

## Chapter 3

# Diversity in OFDMA

In this chapter, we study the diversity characteristic in the frequency-domain. In Sec. 3.1, we first state the assumptions used throughout this thesis, followed by a review of the basic system structure and a framework of the mathematical signal representations of OFDMA. In Sec. 3.2, we derive a mathematical equation that bridges the time-domain diversity and the frequency-domain diversity. From the obtained relationship, a systematic sub-carrier selection method to reach full diversity gain can be drawn for OFDMA transmission. Based on the relationship, a tone-combined OFDMA scheme for transmitters without channel information and a tone-selective OFDMA scheme for transmitters with channel information are discussed respectively in Sec. 3.3 and Sec. 3.4. Their received SNR levels are compared to that of a single-user Rake receiver, and their exact BER expressions are derived for multipath fading channels with Rayleigh distribution.

### 3.1 Assumptions, Structure and Signal Representations

#### 3.1.1 Research Assumptions and A General Structure

For the sake of simplicity, we focus on uncoded and non-equalized system performance. To make the comparison based on the access schemes solely, we assume the possibility of

coherent receivers with perfect frequency and phase recovery. Even though only uplink scenarios are considered in the discussion, our results are applicable to both uplink and downlink OFDMA transmissions.

Fig. 3.1 shows a block diagram of an uplink OFDMA system. The uplink OFDMA

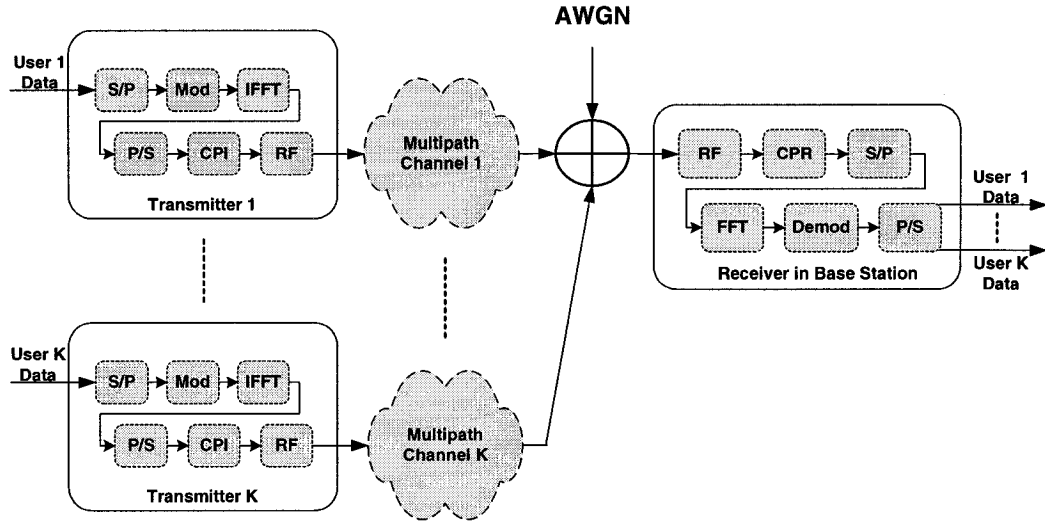


Fig. 3.1 Block diagram of an uplink OFDMA system.

model can be modified to fit into different forms of multi-carrier transmissions.

- For OFDMA with single sub-carrier per user, the 'S/P' block in the transmitter becomes unnecessary.
- Conversely, for OFDMA with multiple sub-carriers per user but the same information transmitted on the sub-carriers, the 'S/P' block in the transmitter is changed to a simple 'Repeater' block.
- For a MC-CDMA structure, the outputs of the 'Repeater' block are multiplied by a spreading sequence.

For all the above cases, corresponding changes also have to be made in the receiver.

### 3.1.2 Signal Representations

As shown in Fig. 3.1, frequency-domain to time-domain transformation of information bearing signals is done by the IFFT operation with user specific frequencies. Without loss of generality, let's consider an OFDMA system with  $N$ -point FFT and  $K$  active users. The transmitted signal of user  $k$  at symbol interval  $n$  can be written as

$$s_{k,n}(t) = \sum_{i=0}^{N+L_{CPI}-1} s_{k,n,i} P_T(t - iT) \quad (3.1)$$

where  $L_{CPI}$  is the length of the CPI,  $\{s_{k,n,i+L_{CPI}}\}$  are the output samples of the IFFT,  $\{s_{k,n,i} \doteq s_{k,n,i+N}, i = 0, 1, \dots, L_{CPI} - 1\}$  is the cyclic prefix portion of the signal, and  $T$  is the sampling interval. The output samples of the IFFT,  $\{s_{k,n,i+L_{CPI}}\}$ , are generated by

$$s_{k,n,i+L_{CPI}} = \mathcal{A}_k \sum_{m=0}^{N-1} S_{k,n,m} C_{k,n,m} e^{j2\pi m i/N}, \quad i = 0, 1, \dots, N-1 \quad (3.2)$$

where  $\mathcal{A}_k \doteq \sqrt{E_k/(N_o N_p)}$  is the signal amplitude,  $E_k$  is the transmitted symbol energy of user  $k$ ,  $N_o$  is the power spectrum density of white Gaussian noise, and  $N_p = N + L_{CPI}$  is the total number of samples in an OFDMA symbol.  $S_{k,n,m}$  is the  $n$ -th symbol of user  $k$  at sub-carrier  $m$ , and with unit energy  $\frac{1}{2}E\{|S_{k,n,m}|^2\} = 1$ .  $C_{k,n,m}$  is a sub-carrier allocation function with value of 1 if the  $m$ -th sub-carrier is allocated for user  $k$  and symbol  $n$ , and with value of 0 otherwise. To avoid any collision, the system should be coordinated such that there is only one  $C_{k,n,m}$  being set to 1 for any given  $n$  and  $m$ .

After passing through distinct  $L_{k,t}$ -multipath channels, signals of all active users arrive at the receiver with different time delays  $\tau_{k,l}$  and experience various multipath fading  $\alpha_{k,l}$ . The received samples after cyclic prefix removal can be represented as

$$V_{n,i} = \sum_{k=1}^K \sum_{l=0}^{L_t-1} \beta_{k,l} s_{k,n,i-l} + \eta_{n,i}, \quad i = L_{CPI}, L_{CPI} + 1, \dots, L_{CPI} + N - 1 \quad (3.3)$$

where  $\eta_{n,i}$  is a zero-mean, unit-variance Gaussian distributed random variable;  $\{\beta_{k,l}\}$  is the equivalent fading parameters transformed from  $\{\alpha_{k,l}\}$ . With predefined  $v_{k,l} \doteq \lceil \tau_{k,l}/T \rceil$ ,  $L_t = \max_{l \in [1, 2, \dots, L_{k,t}]} (v_{k,l} + 1)$  is the number of taps of the transformed channel model. As shown in [29],  $[\beta_{k,0}, \beta_{k,1}, \dots, \beta_{k,L_t-1}]^T = \mathcal{F}_k \cdot [\alpha_{k,1}, \alpha_{k,2}, \dots, \alpha_{k,L_{k,t}}]^T$ , where  $\mathcal{F}_k$  is an  $L_t \times L_{k,t}$  transformation matrix with the  $ij$ -th entry ( $i = 0, 1, \dots, L_t - 1$ ,  $j = 1, 2, \dots, L_{k,t}$ ) denoted by  $\mathcal{F}_{k,i,j}$ . The elements in  $\mathcal{F}_k$  are set to zero except for  $\mathcal{F}_{k,v_{k,l}-1,l}$  and  $\mathcal{F}_{k,v_{k,l},l}$  that are set to  $(T - \tau'_{k,l})$  and  $\tau'_{k,l}$  respectively with  $\tau'_{k,l} \doteq \tau_{k,l} - (v_{k,l} - 1)T$ . After the transformation,  $\{\beta_{k,l}\}$  represent the weights of a channel model whose taps are spaced by sampling interval  $T$ . This channel model simplifies the receiver design as we no longer need to resolve  $L_{k,t}$  paths with arbitrary time spacing. The original multipath fading channel with arbitrary time delays  $\{\tau_{k,l}\}$  is represented by a tapped delay-line model as in Eq. (3.3).

After the serial-to-parallel conversion, the received samples  $\{V_{n,i}\}$  are fed into the FFT block in order to restore the transmitted information-bearing symbol on each sub-carrier. If the length of cyclic prefix is longer than the largest delay, the linear convolutions of  $\beta_{k,l}$  and  $s_{k,n,i}$  are rendered to be the same as the circular convolutions despite various timing offset on each user. Such a cyclic property is maintained in the linear summation of all  $K$  users' signals in  $\{V_{n,i}\}$ . This justifies the use of the FFT. Taking the FFT on both sides of Eq. (3.3) and using  $s_{k,n,i+L_{CPI}}$  in Eq. (3.2), we have

$$Y_{n,m} = \sum_{k=1}^K \mathcal{A}_k N [H_{k,m} \cdot S_{k,n,m} \cdot C_{k,n,m}] + W_{n,m} \quad (3.4)$$

with  $Y_{n,m}$ ,  $H_{k,m}$  and  $W_{n,m}$  denote the  $m$ -th FFT outputs of  $\{V_{n,i}\}$ ,  $\{\beta_{k,l}\}$  and  $\{\eta_{n,i}\}$



respectively, i.e.,

$$Y_{n,m} \doteq \sum_{i=0}^{N-1} V_{n,i+L_{CPI}} e^{-j 2 \pi i m / N} \quad (3.5)$$

$$H_{k,m} \doteq \sum_{l=0}^{L_t-1} \beta_{k,l} e^{-j 2 \pi l m / N} \quad (3.6)$$

$$W_{n,m} \doteq \sum_{i=0}^{N-1} \eta_{n,i+L_{CPI}} e^{-j 2 \pi i m / N} \quad (3.7)$$

For statistically independent and identically distributed (i.i.d.) Gaussian noise samples  $\{\eta_{n,i}\}$  with zero-mean and unit-variance, the FFT transformed noise components  $\{W_{n,m}\}$  are also with Gaussian distribution since  $\{W_{n,m}\}$  are linear combinations of  $\{\eta_{n,i}\}$ . The mean, variance and correlation values of  $\{W_{n,m}\}$  can be calculated as follows.

$$\begin{aligned} E[W_{n,m}] &= E \left[ \sum_{i=0}^{N-1} \eta_{n,i+L_{CPI}} e^{-j 2 \pi i m / N} \right] \\ &= \sum_{i=0}^{N-1} E[\eta_{n,i+L_{CPI}}] e^{-j 2 \pi i m / N} \\ &= 0 \end{aligned} \quad (3.8)$$

$$\begin{aligned} \frac{1}{2} E[W_{n_1,m_1} W_{n_2,m_2}^*] &= \frac{1}{2} \sum_{i_1=0}^{N-1} \sum_{i_2=0}^{N-1} E[\eta_{n_1,i_1+L_{CPI}} \eta_{n_2,i_2+L_{CPI}}^*] e^{-j 2 \pi i_1 m_1 / N} e^{j 2 \pi i_2 m_2 / N} \\ &= \begin{cases} \frac{1}{2} \sum_{i_1=0}^{N-1} E[\eta_{n_1,i_1+L_{CPI}} \eta_{n_1,i_1+L_{CPI}}^*] e^{-j 2 \pi i_1 (m_1 - m_2) / N} & \text{if } n_1 = n_2 \\ 0 & \text{if } n_1 \neq n_2 \end{cases} \\ &= \begin{cases} N & \text{if } n_1 = n_2 \text{ and } m_1 = m_2 \\ 0 & \text{else} \end{cases} \\ &= \begin{cases} N & \text{if } \{n_1, m_1\} = \{n_2, m_2\} \\ \frac{1}{2} E[W_{n_1,m_1}] E[W_{n_2,m_2}] & \text{if } \{n_1, m_1\} \neq \{n_2, m_2\} \end{cases} \end{aligned} \quad (3.9)$$

$\{W_{n,m}\}$  are shown to be uncorrelated, hence they are i.i.d. Gaussian random variables

with mean of 0 and variance of  $N$ .

Eq. (3.4) indicates that as long as the cyclic prefix is long enough to cover the spurious interference duration, OFDMA can retain the orthogonality of  $N$  sub-carriers even in a multipath fading environment. With cooperative sub-carrier allocation scheme  $C_{k,n,m}$ , all  $K$  active users can share the  $N$  available sub-carriers for uplink access as discussed in [30].

### 3.2 Diversity Equivalence in Time- and Frequency-Domains

We have shown in the previous section that OFDMA achieves interference-free transmission. However, the system performance is still limited by the fading characteristic of wireless channels since severe fading conditions can distort signal waveforms. Diversity-protected transmission is required to combat fading. To see how we can achieve full diversity gain efficiently in frequency domain, we study the properties of  $H_m$  for an arbitrary user. The study is general enough so that the result is applicable to any user and under any fading environment.

#### 3.2.1 Theorem on Diversity Equivalence

Conditioned on the channel weights  $\{\beta_l\}$ , the Fourier transformed samples  $H_m$  can be written as the samples of one continuous waveform  $H(t)$ , i.e.,

$$H_m = H(t) |_{t=mT_s} = \sum_{l=0}^{L_t-1} \beta_l e^{-j2\pi l \Delta f t} |_{t=mT_s} \quad (3.10)$$

where  $\Delta f$  is the sub-carrier interval, and  $T_s = 1/(N\Delta f)$  is the sampling interval. If we only take samples of  $H(t)$  at  $L_f$  time instants  $\{t_i = (m_o + i \cdot N/L_f)T_s\}$ , where  $i = 0, 1, \dots, L_f - 1$ , and  $m_o = 0, 1, \dots, \lfloor N/L_f \rfloor - 1$  to ensure the samples are within the

observation interval  $[0, NT_s)$ , then the squared sum of  $L_f$  samples is calculated by

$$\begin{aligned}
\sum_{i=0}^{L_f-1} |H((m_o + i \cdot N/L_f)T_s)|^2 &= \sum_{i=0}^{L_f-1} \left[ \sum_{l_1=0}^{L_t-1} \beta_{l_1} e^{-j 2 \pi l_1 \Delta f t} \Big|_{t=(m_o+iN/L_f)T_s} \right] \\
&\quad \left[ \sum_{l_2=0}^{L_t-1} \beta_{l_2} e^{-j 2 \pi l_2 \Delta f t} \Big|_{t=(m_o+iN/L_f)T_s} \right]^* \\
&= \sum_{i=0}^{L_f-1} \sum_{l_1=0}^{L_t-1} \sum_{l_2=0}^{L_t-1} \beta_{l_1} \beta_{l_2}^* e^{-j 2 \pi (l_1-l_2)(m_o+iN/L_f)/N} \\
&= \sum_{l_1=0}^{L_t-1} \sum_{l_2=0}^{L_t-1} \beta_{l_1} \beta_{l_2}^* e^{-j 2 \pi (l_1-l_2)m_o/N} \sum_{i=0}^{L_f-1} e^{-j 2 \pi (l_1-l_2)i/L_f} \\
&= L_f \sum_{l=0}^{L_t-1} |\beta_l|^2
\end{aligned} \tag{3.11}$$

For  $|l_1 - l_2| < L_f$ , the value of  $\sum_{i=0}^{L_f-1} e^{-j 2 \pi (l_1-l_2)i/L_f}$  equals  $L_f$  only if  $l_1 = l_2$ , and equals 0 otherwise. This explains how the last step of the above equation is derived. Because  $\max(|l_1 - l_2|) = L_t - 1$ , this means the condition  $L_t \leq L_f$  must be satisfied. Based on the above derivation, we introduce the following theorem that shows the diversity equivalence in time-domain and frequency-domain.

**Theorem 1** *Given a multipath fading model with a sample spacing and length  $L_t$ , i.e.,  $\{\beta_l, l = 0, 1, \dots, L_t - 1\}$ , and its DFT  $H_m \doteq \sum_{l=0}^{L_t-1} \beta_l e^{-j 2 \pi l m/N}$  for  $m = 0, 1, \dots, N - 1$ , the following equation holds if  $L_f \geq L_t$ .*

$$\frac{1}{L_f} \sum_{i=0}^{L_f-1} |H_{(m_o + [i \cdot N/L_f])}|^2 = \sum_{l=0}^{L_t-1} |\beta_l|^2 \tag{3.12}$$

where  $m_o$  is an arbitrary choice within  $[0, N/L_f)$ , and  $[\cdot]$  denotes the rounding operation.

If  $L_f$  is not divisible by  $N$ , the equal sign “=” in the equation becomes an approximation “ $\approx$ ”. Fig. 3.2 shows the combined energy ratio of frequency-domain to time-domain,  $\left[ \frac{1}{L_f} \sum_{i=0}^{L_f-1} |H_{(m_o + [i \cdot N/L_f])}|^2 \right] / \left[ \sum_{l=0}^{L_t-1} |\beta_l|^2 \right]$ , in a 5-tap exponential decaying

channel model. The value of  $L_f$  is set to 5, and the number of sub-carriers  $N$  varies

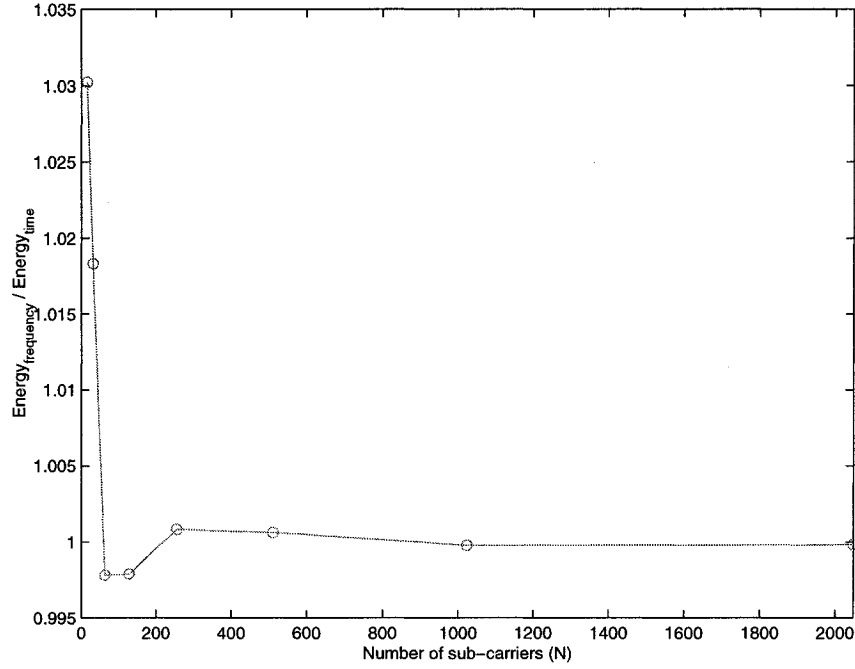


**Fig. 3.2** Energy ratio for  $L_f$  not divisible by  $N$

from 16 to 2048. The example shows that the approximation becomes more accurate when the value of  $N$  is large.

Overall, Theorem 1 indicates:

- In multi-carrier transmissions, by assigning  $L_f (\geq L_t)$  sub-carriers with  $N/L_f$  sub-carriers apart to a user, each assigned sub-carrier bears  $1/L_f$  of the user's energy.
- If their energies are combined in frequency-domain, its sum equals to the square sum of the time-domain fading replicas, i.e.,  $\{\beta_l\}$ .
- While achieving the same combining as in the time-domain Rake receiver, the system spectral efficiency is decreased due to the fact that the same data is transmitted on more than one sub-carriers.

If a sub-carrier group is composed of the  $L_f$  sub-carriers required to obtain the full diversity gain, Fig. 3.3 shows the formation of a sub-carrier group within a system

spectrum.

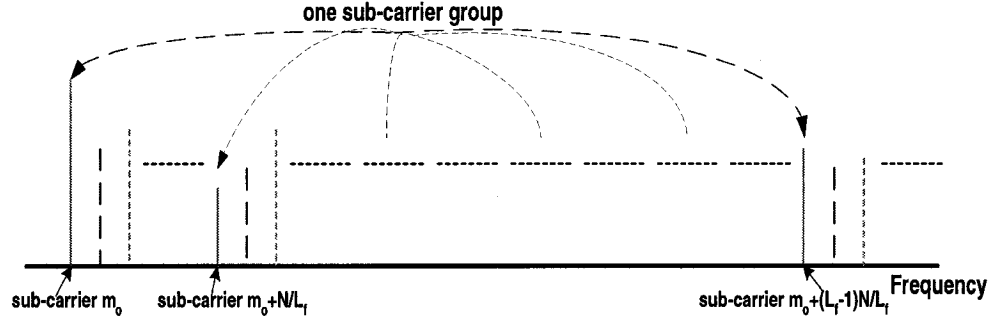


Fig. 3.3 The formation of sub-carrier group

### 3.2.2 Criteria on Selection of $L_f$

To minimize the degradation on spectral efficiency, the least number of sub-carriers should be occupied by a user. On the other hand, we want the full diversity gain on all users regardless of the value of  $N$ . This requires the selection of the least value of  $L_f$  to be both divisible, and larger than  $L_t$  at the same time in practical system design. Based on the fact that  $N$  is the number of points used in FFT operation, we define the following criteria for the selection of  $L_f$ .

**Criteria 1** *For full diversity gain, and minimum spectral efficiency degradation, the choice of the number of sub-carriers per user,  $L_f$ , must fulfill*

- I.  $L_f$  must be not less than the number of multipath  $L_t$ .
- II.  $L_f$  is the minimum power of 2 that satisfies Criterion I.

Criterion II also enables us to incorporate orthogonal spreading sequences into the design as it will be shown in Chapter 5. By obeying the above criteria,  $L_f$  has the minimum allowable value guaranteed to be divisible, and the relation mentioned in Theorem 1 is always exact. To select sub-carrier group, the initial variable  $m_o$  can be regarded as a

user index. Even different users have distinct sub-carrier groups, the formation of the sub-carrier groups require the same mechanics for all users. To make use of Theorem 1 for transmission techniques, we have to discuss two categories of transmissions. One is the case that channel information is not available to transmitters, and the other is that transmitters know about the channel. Multiple-access techniques will be developed separately for these two categories.

### **3.3 Tone-Combined Technique without Channel Information at Transmitters**

In most applications, transmitters do not know channel information. This is mainly due to two reasons. One is because of the limited computational power on mobile stations. The other is due to the fast time-varying characteristic of the channel. The design of mobile station is constrained by the size of handset and the life of battery, and hence complex channel acquisition algorithm should not be supported on mobile stations. One way to get around this is to acquire channel information on base stations, and then transmit the information back to mobile stations. Unfortunately, in such a scenario, even if accurate channel information is known, by the time the information gets back to transmitters and an adaptive algorithm is implemented, the channel conditions may have already changed. So there is always a time lag between the acquisition and the implementation. Depending on how fast the channel changes, the situation of having a time lag may be equivalent to the case of no channel information available.

#### **3.3.1 TC-OFDMA**

For transmitters without channel information, techniques to combat fading have to be used. Assume the modulation technique and the bandwidth of each sub-carrier are designed such that only one sub-carrier per user is needed to satisfy the data rate re-

quirement of the users. Theorem 1 in Sec. 3.2 shows us how to obtain the full diversity by using multiple sub-carriers. With the selection of  $L_f$  satisfying Criteria 1 in Sec. 3.2, we propose the following tone (sub-carrier) combined OFDMA (TC-OFDMA) technique for the case when the number of active users is less than  $N/L_f$ .

In TC-OFDMA, each user occupies a group of sub-carriers with indices  $\{m_i = m_o + [iN/L_f], i = 0, 1, \dots, L_f - 1\}$ , where  $m_o$  ( $0 \leq m_o \leq N/L_f - 1$ ) is a user index. At the receiver, a frequency-domain Rake receiver in [31] is adopted to combine the received samples  $\{Y_{n,m_i}\}$  over  $\{m_i, i = 0, 1, \dots, L_f - 1\}$  tones. By assuming perfect channel knowledge at the receiver, the resulting decision variable can be represented by

$$\begin{aligned} D_k &= \sum_{i=0}^{L_f-1} H_{k,m_i}^* Y_{n,m_i} \\ &= \frac{1}{\sqrt{L_f}} \mathcal{A}_k N S_{k,n,m} \sum_{i=0}^{L_f-1} |H_{k,m_i}|^2 + \sum_{i=0}^{L_f-1} H_{k,m_i}^* W_{n,m_i} \end{aligned} \quad (3.13)$$

where  $1/\sqrt{L_f}$  is the normalized factor applied to keep the transmitted signal power constant,  $C_{k,n,m_i}$  is 1, and  $S_{k,n,m}$  is taken out from the summation since it is the same for all  $m_i$ . By applying the diversity equivalence in Theorem 1, the signal-to-noise ratio (SNR) of user  $k$  with equal-power distribution over  $L_f$  tones, denoted by  $\gamma_k$ , is

$$\begin{aligned} \gamma_k &= \frac{1}{L_f} \mathcal{A}_k^2 N \sum_{i=0}^{L_f-1} |H_{k,m_i}|^2 \\ &= \frac{N}{N_p} \frac{E_k}{N_o} \sum_{l=0}^{L_t-1} |\beta_{k,l}|^2 \end{aligned} \quad (3.14)$$

From the above equation, we can see that the received signal combines energies from all paths. The SNR is the same as the one achieved by the Rake receiver in a single-user CDMA system except for a small energy loss due to the cyclic prefix. This result not only confirms the idea of frequency spreading along the system spectrum to mitigate the frequency-selective fading [1], but also points out that with a choice of  $L_f$  that satisfies

Criteria 1, all users can accomplish the error rate performance of a single-user time-domain Rake receiver with a minimum number of sub-carriers per user. The penalty to pay is a slightly higher peak to average power ratio (PAR) ( $\doteq 10\log L_f$  dB).

### 3.3.2 BER Analysis

With performance of a single-user time-domain Rake receiver, the BER of TC-OFDMA with M-ary QAM modulation can be derived in multipath frequency-selective Rayleigh fading channel. From Eq. (3.14), the average received SNR per bit can be calculated as

$$\begin{aligned}\bar{\gamma}_{b,k} &= \frac{E_{b,k}}{N_o} \frac{N}{N_p} \sum_{l=0}^{L_t-1} |\beta_{k,l}|^2 \\ &= \sum_{l=0}^{L_t-1} \bar{\gamma}_{b,k,l}.\end{aligned}\quad (3.15)$$

The instantaneous SNR of an individual path is a function of  $|\beta_{k,l}|^2$ , where  $\beta_{k,l}$  is function of  $\alpha_{k,l}$ . If  $\alpha_{k,l}$  are i.i.d. complex Gaussian variables with Rayleigh distributed amplitude, and with delay profile coinciding with the sampling interval spacing,  $\beta_{k,l}$  are also i.i.d. complex Gaussian variables with Rayleigh distributed amplitude. Therefore,  $|\beta_{k,l}|^2$  has a chi-square probability density function, and so does the instantaneous SNR of an individual path. Eq. (14.5-26) in [32] shows that the probability density function of the instantaneous SNR,  $\gamma_{b,k}$ , for  $[L_t - 1]$  independent paths with unequal powers is  $p(\gamma_{b,k}) = \sum_{l=0}^{L_t-1} \frac{\pi_{k,l}}{\bar{\gamma}_{b,k,l}} e^{-\frac{\gamma_{b,k}}{\bar{\gamma}_{b,k,l}}}$ , where  $\pi_{k,l} = \prod_{i=0, i \neq l}^{L_t-1} \frac{\bar{\gamma}_{b,k,l}}{\bar{\gamma}_{b,k,l} - \bar{\gamma}_{b,k,i}}$ .

On the other hand, the conditional bit error probability for M-ary QAM signaling is in the form of [33]

$$P_b(e|\gamma_{b,k}) = \frac{1}{\log_2(I \cdot J)} \left( \sum_{a=1}^{\log_2 I} P_I(a) + \sum_{b=1}^{\log_2 J} P_J(b) \right) \quad (3.16)$$



where  $I$  and  $J$  are the dimensions of the corresponding PAM signals, and

$$P_I(a) = \frac{1}{I} \sum_{c=0}^{(1-2^{-a})I-1} \left\{ (-1)^{\lfloor \frac{c \cdot 2^{a-1}}{I} \rfloor} \left[ 2^{a-1} - \left\lfloor \frac{c \cdot 2^{a-1}}{I} + \frac{1}{2} \right\rfloor \right] \cdot \operatorname{erfc} \left[ (2c+1) \sqrt{\frac{3 \log_2(I \cdot J) \gamma_{b,k}}{I^2 + J^2 - 2}} \right] \right\} \quad (3.17)$$

$$P_J(b) = \frac{1}{J} \sum_{c=0}^{(1-2^{-b})J-1} \left\{ (-1)^{\lfloor \frac{c \cdot 2^{b-1}}{J} \rfloor} \left[ 2^{b-1} - \left\lfloor \frac{c \cdot 2^{b-1}}{J} + \frac{1}{2} \right\rfloor \right] \cdot \operatorname{erfc} \left[ (2c+1) \sqrt{\frac{3 \log_2(I \cdot J) \gamma_{b,k}}{I^2 + J^2 - 2}} \right] \right\} \quad (3.18)$$

The average bit error rate is then obtained by  $P_b = \int_0^\infty P_b(e|\gamma_{b,k}) p(\gamma_{b,k}) d\gamma_{b,k}$ . By evaluating the integral in the same way as Eq. (14.5-28) in [32], a closed-form for the BER can be expressed as

$$P_b = \frac{1}{\log_2(I \cdot J)} \left\{ \sum_{a=1}^{\log_2 I} \frac{1}{I} \sum_{c=0}^{(1-2^{-a})I-1} [\Theta(c, a, I) \cdot \Omega(c, I, J)] + \sum_{b=1}^{\log_2 J} \frac{1}{J} \sum_{c=0}^{(1-2^{-b})J-1} [\Theta(c, b, J) \cdot \Omega(c, I, J)] \right\} \quad (3.19)$$

where

$$\Omega(a, b, c) = \sum_{l=0}^{L_t-1} \pi_{k,l} \left[ 1 - \sqrt{\frac{\bar{\gamma}_{b,k,l} \cdot 2\aleph(a, b, c)}{2 + \bar{\gamma}_{b,k,l} \cdot 2\aleph(a, b, c)}} \right], \quad (3.20)$$

$$\aleph(a, b, c) = \frac{3(2a+1)^2 \log_2(bc)}{b^2 + c^2 - 2}, \quad (3.21)$$

$$\Theta(a, b, c) = (-1)^{\lfloor \frac{a \cdot 2^{b-1}}{c} \rfloor} \left[ 2^{b-1} - \left\lfloor \frac{a \cdot 2^{b-1}}{c} + \frac{1}{2} \right\rfloor \right]. \quad (3.22)$$

Obviously, Eq. (3.19) can be easily computed to obtain the BER of TC-OFDMA system with M-ary QAM signaling over multipath frequency-selective Rayleigh fading channels. To confirm the result, we set  $I=2$  and  $J=1$ , i.e., BPSK signaling, the BER expression is

reduced to the well known result of Eq. (14.5-28) in [32]. In addition, we simulate the BER performances for 8, 16, 32 and 64 QAM. Fig. 3.4 shows a good agreement between the analytical and simulation results for higher M-ary QAM over a two-tap Rayleigh channel with power profile [0,-6]dB.

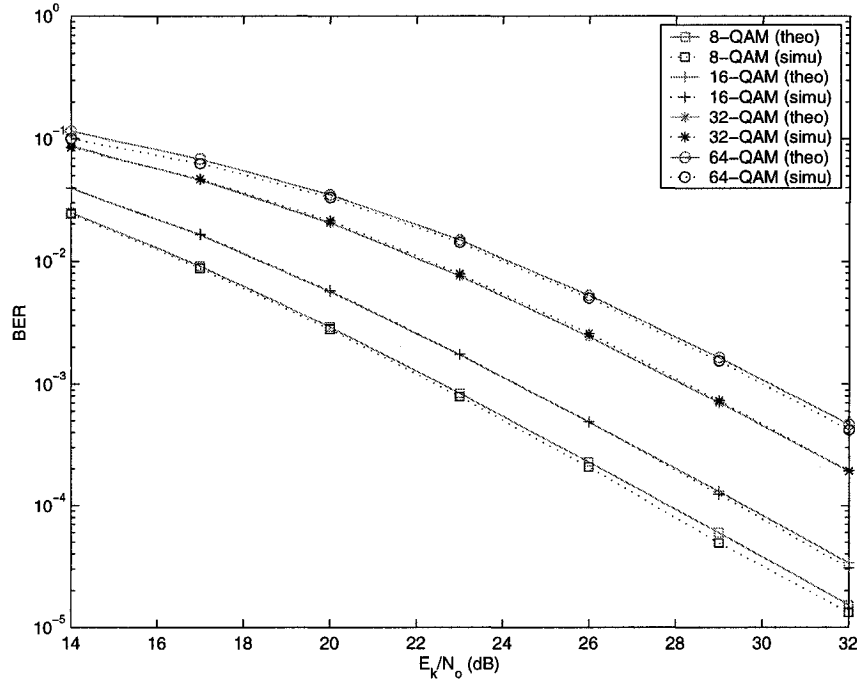


Fig. 3.4 BER performance of TC-OFDMA with various M-ary QAM

### 3.4 Tone-Selective Technique with Channel Information at Transmitters

#### 3.4.1 TS-OFDMA

For transmitters without channel information, the tone-combined technique has successfully combated the multipath fading by using multiple sub-carriers. With symbol energy split into the assigned sub-carrier group, the TC-OFDMA scheme achieves the performance of a Rake receiver in the single-user CDMA system. However, since symbol energy has to be divided evenly into all its sub-carriers, a waste of symbol energy is

inevitable as bad sub-carriers have the same weight as good sub-carriers. If channel information is known in advance, signal energy can be concentrated on the best sub-carrier to avoid any energy waste.

In a time-invariant or slowly time-varying channel, with channel knowledge available to transmitters, the technique of selecting the best member of the sub-carrier group is more efficient than the technique of combining all members [34]. Based on the above reasoning, we propose a tone-selective OFDMA (TS-OFDMA) scheme for transmitters with channel information. We make the same assumptions as in the last section, i.e., the number of active users is less than  $N/L_f$ , and one sub-carrier per user satisfies the data rate requirement. As one user still occupies the whole sub-carrier group, the TS-OFDMA differs from the TC-OFDMA in the number of sub-carriers used for transmissions. Specifically, there is no normalized factor for the received symbol energy since TS-OFDMA chooses only the best sub-carrier among each group. For any given  $m_o$ , the best sub-carrier in the group has the largest power as shown in the following inequality.

$$\begin{aligned}
 \max_{i \in \{0, 1, \dots, L_f - 1\}} \{|H_{k, m_o + [i \cdot N/L_f]}|^2\} &= |H_{k, m_o + [i' \cdot N/L_f]}|^2 \\
 &\geq \frac{1}{L_f} \sum_{i=0}^{L_f-1} |H_{(m_o + [i \cdot N/L_f])}|^2 \\
 &\geq \sum_{l=0}^{L_t-1} |\beta_{k, l}|^2
 \end{aligned} \tag{3.23}$$

With the best sub-carrier  $m_{i'} = m_o + [i' \cdot N/L_f]$  selected, the decision variable and the resulting SNR of TS-OFDMA can be represented by the following two expressions.

$$\begin{aligned}
 D_k &= H_{k, m_{i'}}^* Y_{n, m_{i'}} \\
 &= \mathcal{A}_k N S_{k, n, m} |H_{k, m_{i'}}|^2 + H_{k, m_{i'}}^* W_{n, m_{i'}}
 \end{aligned} \tag{3.24}$$

$$\gamma_k = \mathcal{A}_k^2 N |H_{k, m_{i'}}|^2 \tag{3.25}$$

### 3.4.2 BER Analysis

By assuming an equal power profile, a sample spacing delay profile, and the i.i.d. complex Gaussian fading parameters  $\{\alpha_{k,l}\}$  with Rayleigh distributed amplitude, the DFT outputs,  $H_{k,m}$ , are also i.i.d. complex Gaussian variables with mean of zero, and variance of  $\sum_{l=0}^{L_t-1} \mathbf{E}|\alpha_{k,l}|^2$ . By choosing  $L_f$  sub-carriers for selection diversity, the SNR improvement offered by the proposed tone selective technique over randomly choosing a single tone is evaluate by Eq. (6.62) of [6],  $\gamma_k/\Gamma = \sum_{l=1}^{L_f} 1/l$ , where  $\Gamma = \mathcal{A}_k^2 N \sum_{l=0}^{L_t-1} \mathbf{E}|\alpha_{k,l}|^2$  is the average SNR of each tone. The probability density function of the received SNR with selection diversity can be derived by using the same process as in Sec. 6.10.1 of [6].

$$p(\gamma_k) = \frac{L_f}{\Gamma} e^{-\gamma_k/\Gamma} (1 - e^{-\gamma_k/\Gamma})^{L_f-1} \quad (3.26)$$

On the other hand, the conditional bit error probability for M-ary QAM signaling is defined by Eq. (3.16). With the same probability density function as  $\gamma_k$  for the received SNR per bit  $\gamma_{b,k}$ , the average BER in Rayleigh fading channel can be calculated by  $P_b = \int_0^\infty P_b(e|\gamma_{b,k}) p(\gamma_{b,k}) d\gamma_{b,k}$ . The derivation is shown in Appendix A and it confirms that the average BER of TS-OFDMA has the same closed-form expression as that of TC-OFDMA, i.e.,

$$P_b = \frac{1}{\log_2(I \cdot J)} \left[ \sum_{a=1}^{\log_2 I} \frac{1}{I} \sum_{c=0}^{(1-2^{-a})I-1} \Theta(c, a, I) \cdot \Omega(c, I, J) + \sum_{b=1}^{\log_2 J} \frac{1}{J} \sum_{c=0}^{(1-2^{-b})J-1} \Theta(c, b, J) \cdot \Omega(c, I, J) \right] \quad (3.27)$$

where  $\Theta(a, b, c)$  is the same as that defined by Eq. (3.22), but

$$\Omega(a, b, c) = \sum_{i=0}^{L_f} \binom{L_f}{i} \cdot (-1)^i \sqrt{\frac{\aleph(a, b, c)}{\aleph(a, b, c) + i(b^2 + c^2 - 2)}} \quad (3.28)$$

$$\aleph(a, b, c) = 3\Gamma_b(2a+1)^2 \log_2(bc) \quad (3.29)$$

$$\Gamma_b = \Gamma / \log_2 M \quad (3.30)$$

Calculation of Eq. (3.27) can be done readily to obtain the BER of TS-OFDMA scheme over equal-power multipath frequency-selective Rayleigh fading channels. One can check that by setting  $I=2$  and  $J=1$ , i.e., BPSK signalling, the BER expression is the same as Eq. (14) of [35] and Eq. (13) of [36]. For higher M-ary QAM, Fig. 3.5 compares the analytical and simulation results over a 2-tap equal-power Rayleigh fading channel, and shows an excellent agreement between them. This justifies the correctness of our BER derivation.

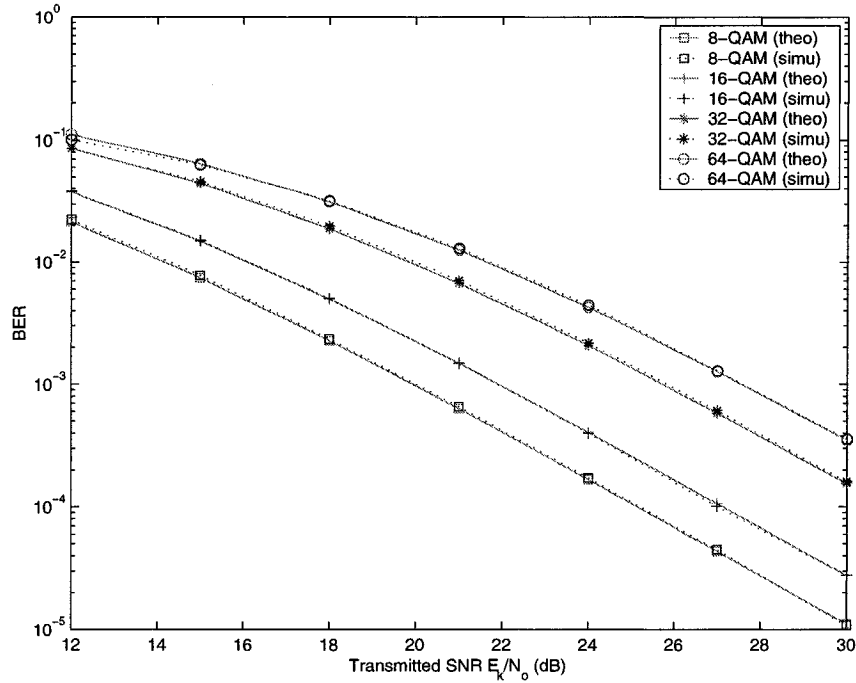


Fig. 3.5 BER performance of TS-OFDMA with various M-ary QAM.

### 3.5 Chapter Summary

In this chapter, we reviewed the assumptions, the system structure and the signal representations for our researches. We proposed a theorem that not only proves the diversity equivalence between time-domain and frequency-domain transmissions, but also shows a systematic approach to achieve the full diversity with multiple sub-carriers. A criteria to select the minimum number of sub-carrier to achieve the exact full diversity for all users was also given. Based on the theorem and the criteria, we suggested a TS and a TC techniques for the cases of with and without channel information respectively. The TC technique helps OFDMA to achieve the single-user Rake receiver's performance, while the TS technique has superior performance than the single-user Rake receiver. Closed-form BER expressions were derived for the two techniques in Rayleigh fading channels as well. However, one drawback for both techniques is the limited number of active users. To support more users, the next two chapters develop the two techniques further in an aim of maximizing spectral efficiency.

## Chapter 4

### Group-Optimal

### Adaptive-Tone-Diversity (GO-ATD)

### OFDMA for Transmitters with

### Channel Information

In slowly time-varying channels, it can be assumed that transmitters have enough time to seize channel information and adapt the suitable modulation scheme accordingly. The adaptation can be either constrained on the transmitted power or the data rate. In most data transmissions, the transmitted powers have caps, while data rates can vary. In such a scenario, bit-loading on each sub-carrier can enhance the system performance.

In this chapter, to improve the spectral efficiency of the tone-selective technique, we propose a group-optimal adaptive-tone-diversity OFDMA (GO-ATD-OFDMA) scheme. The scheme applies adaptive tone diversity and bit-loading technique on each sub-carrier. By controlling each individual data rate, similar error rate performances are expected on both good and bad sub-carriers. The adaptive scheme provides both diversity-protected and interference-free transmission.

To facilitate our discussions, we first introduce in Sec. 4.1 the bit-loading technique to support M-ary QAM from  $M = 2$  (BPSK) to  $M = 512$ . With our assumption of one sub-carrier per user, user's power is poured into its assigned sub-carrier only, and hence power allocation is not an concern in our scheme. Moreover, while we follow the same procedure as in [37] to derive the bit-loading formula, we consider more details by having separate discussions of rectangular QAM, square QAM and BPSK. Then in Sec. 4.2, we explain the GO-ATD-OFDMA structure and show how it realizes the optimal resource allocation within each sub-carrier group. In Sec. 4.3, the system performances in terms of error rate and throughput are examined, and the effect of inaccurate channel estimation is studied.

#### **4.1 Bit-Loading Technique with M-ary QAM**

By controlling the modulation scheme on each sub-carrier, the optimal bit-loading technique under constant power constraint attempts to achieve the required BER on all sub-carriers. A sub-carrier with higher energy is loaded with more bits; and a sub-carrier with lower energy is loaded with less bits. To reach the same BER, iterative computations have to be performed. However, the computations are too complicated for practical systems even in slowly time-varying wireless channels. A much simpler approach to approximate the optimal bit-loading technique can be realized by using SER as the required target in calculating the number of loaded bits.

The reasons why SER can replace BER in the bit-loading computation are given as follows. The BER of M-ary QAM can be approximated by dividing the SER by the number of bits per symbol. If the difference of number of bits per symbol among all sub-carriers is smaller than 10, which is very likely in wireless non-LOS transmissions, then the same SER guarantees all resulting BER have the same order of magnitude. On the other hand, with only quantized levels of M-ary QAM (granularity of 1 bit), even



bit-loading technique using BER calculation cannot achieve exactly the required BER. Therefore, accomplishing the same SER provides us a practical way to approximate the optimal bit-loading technique.

When considering M-ary QAM modulation schemes, we can classify the schemes into two categories: rectangular QAM and square QAM. Unlike the approach in [37], which derives the number of loaded bits by assuming square QAM modulation, we have separate considerations for square QAM and rectangular QAM.

The average symbol energies of the two QAM categories can be calculated as follows. Assuming a unit sampling period, since the average energy of one-dimension o-ary PAM is  $E_{av} = 1/12(o^2 - 1)D_{in}^2$ , where  $o$  is the order of PAM, and  $D_{in}$  is the minimum distance between any two signaling points at the channel input, then for two-dimension M-ary QAM signaling, the  $E_{av}$  can be expressed as a sum of two one-dimension PAM.

$$E_{av} = \frac{1}{12}[(o_r^2 - 1) + (o_i^2 - 1)]D_{in}^2 \quad (4.1)$$

where  $o_r$  and  $o_i$  are the orders of PAM for two dimensions. In square QAM, as  $o_r = o_i = \sqrt{M}$ , the  $E_{av}$  can be simplified as

$$E_{av} = \frac{1}{6}(M - 1)D_{in}^2 \quad (4.2)$$

In rectangular QAM, without loss of generality, we can assume  $o_r = \sqrt{2M}$  and  $o_i = \sqrt{M/2}$ , then its average energy is

$$E_{av} = \frac{1}{6}(1.25M - 1)D_{in}^2 \quad (4.3)$$

One special case is when  $M = 2$  (BPSK), the average energy is represented as

$$E_{av} = \frac{1}{12}(2M - 1)D_{in}^2 \quad (4.4)$$

From the above representations, the value of  $M$  can be found once we know  $E_{av}$ . With  $D_{out}^2 = D_{in}^2 |H_m|^2$  denoting the square of the distance at the channel output, the value of  $M$  for square QAM can be calculated by

$$\begin{aligned} M &= 1 + \frac{6E_{av}}{D_{in}^2} \\ &= 1 + \frac{6E_{av}|H_m|^2}{D_{out}^2} \\ &= 1 + \frac{\gamma_{out}}{\Gamma} \end{aligned} \quad (4.5)$$

where the output SNR  $\gamma_{out}$  is defined as

$$\gamma_{out} = \frac{E_{av}|H_m|^2}{2\sigma^2} \quad (4.6)$$

and the SNR gap  $\Gamma$  is defined as

$$\Gamma = \frac{D_{out}^2}{12\sigma^2} \quad (4.7)$$

By the same process, the value of  $M$  for rectangular QAM and BPSK can be represented respectively by the following two equations.

$$M = \frac{4}{5} \left( 1 + \frac{\gamma_{out}}{\Gamma} \right) \quad (4.8)$$

$$M = \frac{1}{2} + \frac{\gamma_{out}}{\Gamma} \quad (4.9)$$

With Eq. (4.5), Eq. (4.8) and Eq. (4.9) for square QAM, rectangular QAM and BPSK respectively, our representation of  $M$  is more accurate than Eq. (11) alone in [37]. The comparison of Eq. (4.5) and Eq. (4.8) tells us that with the same SNR gap, which implies the same symbol error rate, the rectangular QAM requires extra energy than its counterpart, the square QAM. Table 4.1 shows the required values of  $1 + \frac{\gamma_{out}}{\Gamma}$  for different M-ary modulations.

Since the output SNR is known to transmitters in slowly time-varying channels, we

**Table 4.1** The threshold values for different modulation schemes

$1 + \frac{\gamma_{out}}{F}$	640	256	160	64	40	16	10	4	2.5
M-ary QAM	512	256	128	64	32	16	8	4	2
Number of bits	9	8	7	6	5	4	3	2	1

only need to evaluate the value of the SNR gap to determine the M-ary modulation on each sub-carrier. The SNR gap is related to the required SER of the system. For a square QAM, the SER is approximated by Eq. (7) of [37].

$$P_s \leq 4Q \left[ \frac{D}{2\sigma} \right] \quad (4.10)$$

where  $\sigma^2 = N_o/2$  is the noise variance. For rectangular M-ary QAM, a tight upper-bound of the SER is shown by Eq. (5.2-80) of [32].

$$P_s \leq 4Q \left[ \sqrt{\frac{3E_{av}}{(M-1)N_o}} \right] \quad (4.11)$$

By substituting Eq. (4.3) for  $E_{av}$ , we have

$$\begin{aligned} P_s &\leq 4Q \left[ \sqrt{\frac{(1.25M-1)D^2}{2(M-1)N_o}} \right] \\ &\leq 4Q \left[ \sqrt{\frac{(M-1)D^2}{2(M-1)N_o}} \right] \\ &= 4Q \left[ \frac{D}{2\sigma} \right] \end{aligned} \quad (4.12)$$

As shown, the same SER upper bound is applied for both square and rectangular QAM. However, the bound is loose for rectangular QAM. In addition, we consider only uncoded systems with granularity of 1 bit, so our bit-loading technique will achieve lower SER as we load bits to the smaller but closest integer. Therefore, a factor of 1/2 can be added to the upper bound to have a more accurate estimation with respect to the actual SER.

The use of the  $1/2$  factor will be justified by simulations results in Sec. 4.3.

$$P_s \approx 2Q \left[ \frac{D}{2\sigma} \right] = 1 - \text{erf} \left[ \frac{D}{2\sqrt{2}\sigma} \right] \quad (4.13)$$

or equivalently,

$$\frac{D}{2\sigma} = \sqrt{2} \cdot \text{erf}^{-1}(1 - P_s) \quad (4.14)$$

Substituting the above equation into Eq. (4.7), we have

$$\Gamma = \frac{2}{3} [\text{erf}^{-1}(1 - P_s)]^2 \quad (4.15)$$

The values of SNR gap required for different values of SER are summarized in Table 4.2. With Table 4.1 and Table 4.2 together, we can easily judge what kind of M-ary QAM to use on sub-carriers according to their channel conditions and the required SER target.

**Table 4.2** SNR gaps required for different symbol error rates

$P_s$	$10^{-2}$	$10^{-3}$	$10^{-4}$	$10^{-5}$	$10^{-6}$	$10^{-7}$
$\Gamma(\text{dB})$	3.449	5.579	7.029	8.129	9.019	9.759

## 4.2 Group-Optimal Adaptive-Tone-Diversity OFDMA

In the TS-OFDMA scheme, users can achieve better performances than a single-user Rake receiver. However, with the TS technique, all sub-carriers except one within each sub-carrier group are left unused. In the case of a large number of sub-carriers per sub-carrier group, i.e.,  $L_f$ , the technique might cause a big loss in spectral efficiency. To solve this problem, we try to make use of all leftover sub-carriers by assigning users to them. A user that is first assigned to a sub-carrier group can chose the best sub-carrier for itself. Users that are assigned later have to chose from the leftover sub-carriers. Since each user has distinct channel condition, the best sub-carrier for one user may not the best

sub-carrier for others. Nevertheless, users who have earlier access to a sub-carrier group have better statistical performances than users who have later access. Based on the above intuition, we introduce two processes to assist the utilization of all sub-carriers: one is to prioritize users, and the other is to apply bit-loading on all sub-carriers.

- With a priority on each user, we know the order to assign users into sub-carrier groups. Users with higher priority will be assigned before users with lower priority, and hence obtain larger order of selection diversity. For users in the same priority level, they are uniformly allocated to different sub-carrier groups. In other words, they will be assigned sequentially to the least crowded sub-carrier groups, and obtain the best available sub-carriers within their sub-carrier groups.
- Adaptive bit-loading is applied to all sub-carriers according to the error rate requirement of users. Normally, all users will have the same error rate requirement. In such a case, users with various priorities differ in their transmitted data rates, and hence users should be prioritized based on their data rate requirements. On the other hand, a lower error rate might be required for some important transmissions. In this case, users are prioritized based on their error rate requirements, and users with lower priority may have the same or even higher transmission rates than users with higher priority.

We follow the same procedure in TS-OFDMA to construct the sub-carrier groups, that is,  $N/L_f$  sub-carrier groups are formed, and each sub-carrier group consists of  $L_f$  sub-carriers distributed evenly over the system spectrum. The way to construct the sub-carrier groups guarantees that each group will have the same average channel conditions, and hence users in the same priority level will have similar performance. Furthermore, when the system load is smaller than  $N/L_f$ , all users can have the highest priority, and hence the improvement provided by selection diversity assures that all active users will have better performance than the single-user time-domain Rake receiver.

With users prioritized, the optimal sub-carrier assignment scheme for a user is to select the best available sub-carrier among the whole system spectrum. The complexity of such assignment is  $\mathcal{O}(N^2)$ . In our proposed scheme, the grouping structure reduces the complexity to  $\mathcal{O}(N \cdot L_f)$ . Simulation results in Sec. 4.3 show negligible performance degradation of our scheme as compared to the optimal scheme. Hence, the proposed scheme enhances the OFDMA system performance with reduced computational complexity. Since the best leftover sub-carrier within the least crowded sub-carrier group is always assigned to the appropriate user, the proposed scheme achieves optimal adaptive tone diversity within each sub-carrier group. Therefore, we call it group-optimal adaptive-tone-diversity (GO-ATD) OFDMA.

### 4.3 System Performances

#### 4.3.1 System SER

We assume in our simulations that all users have the same SER requirement. To ensure our bit-loading technique actually delivers the required SER in different channel environments, we examine the actual SER performance in two channel models. The first model is a four-tap Rayleigh fading channel with an exponentially decaying power profile of  $[0, -3.5, -6.9, -10.4]$ dB and a delay profile of  $[0, 0.2, 0.4, 0.6]$  $\mu$ s. With a sampling frequency of 5MHz and a FFT size of 256, the size of sub-carrier group,  $L_f$ , is chosen to be 4. The second model is a typical fixed access broadband wireless channel. The channel is represented by the modified Stanford University Interim (SUI)-3 with a power profile of  $[0, -5, -10]$ dB, a delay profile of  $[0, 0.4, 0.9]$  $\mu$ s, and Rician fading K-factors of  $[1, 0, 0]$  [38]. With the same sampling frequency and FFT size,  $L_t$  in this case is 6, and hence  $L_f$  is chosen to be 8. Fig. 4.1 shows the performance with two different SER requirements,  $10^{-2}$  and  $10^{-3}$  respectively. As shown, even though performance variation exists between the two channel models, their actual SER are still lower than the required

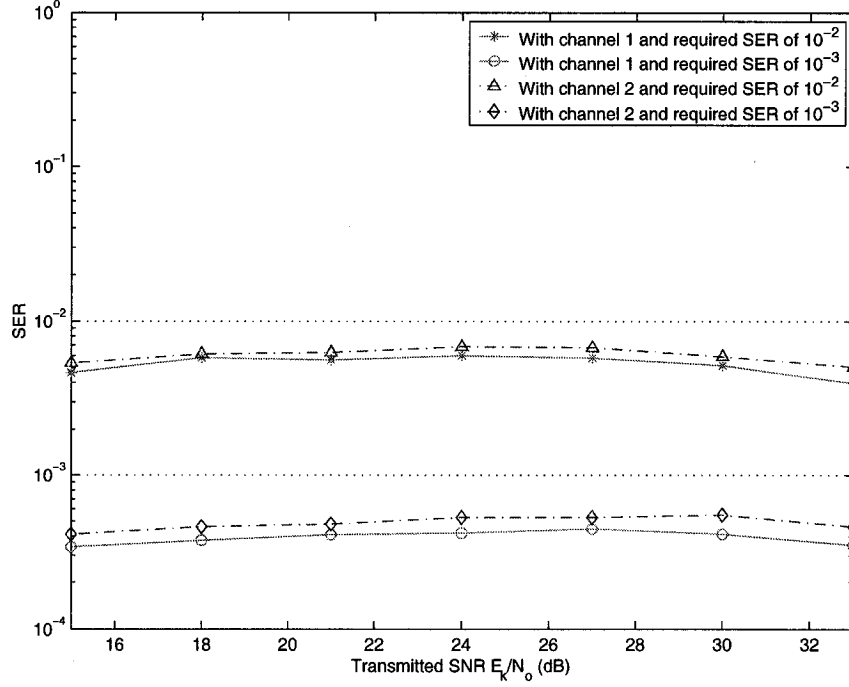


Fig. 4.1 Actual SER with bit-loading technique.

SER. This confirms the multiplication factor of  $1/2$  in Eq. (4.12). The SER difference between the reality and the requirement is mainly due to the large granularity of our uncoded scheme.

#### 4.3.2 System Throughput

To investigate the performance of GO-ATD-OFDMA, we evaluate its achievable system throughput (in b/s/Hz). The system throughput in SUI-3 channel model is compared to the throughput of a random-hop OFDMA (RH-OFDMA) system in Fig. 4.2 at a required SER of  $10^{-2}$ . Users are assumed to have cooperative hopping patterns in the RH-OFDMA system. It is shown that the GO-ATD-OFDMA system has better throughput than the RH-OFDMA system has.

Next, to compare with the optimal sub-carrier assignment scheme, we examine the system throughput,  $S_{GO-ATD}$ , obtained at a given system load of GO-ATD-OFDMA, and take the best throughput obtained with the optimal sub-carrier assignment,  $S_{OPT}$ , as

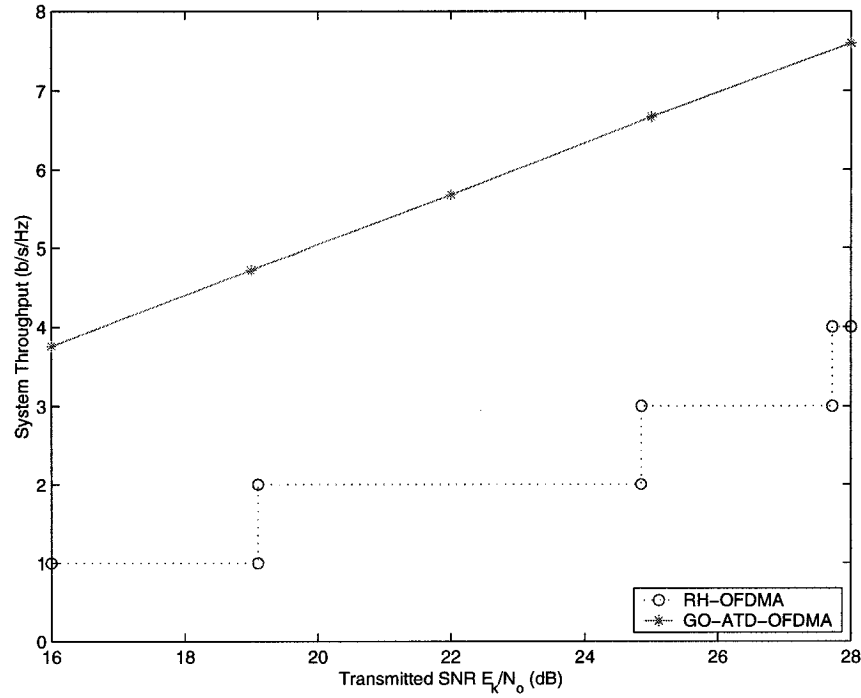


Fig. 4.2 Throughput comparison between GO-ATD-OFDMA and RH-OFDMA.

a reference. The throughput comparison is done with the same simulation parameters as in last example, and a transmitted SNR of 18dB. The ratio of  $S_{GO-ATD}/S_{OPT}$  is shown in Fig. 4.3. Since both systems use the same bit-loading technique, the performance difference is only due to the sub-carrier assignment schemes. The simulation results show the throughput of GO-ATD-OFDMA is slightly degraded, e.g.,  $S_{GO-ATD}/S_{OPT} = 0.927$  at the full load, while its computational complexity is only  $\frac{L_f}{N} = \frac{1}{32}$  of that of the optimal sub-carrier assignment. Re-assignment of the sub-carriers is necessary as channel conditions change with time. With the great reduction in computational complexity, the re-assignment of GO-ATD-OFDMA can be done quickly.

#### 4.3.3 Effects of Erroneous Channel Estimation

We have shown that the system capacity can be maximized with the appropriate sub-carrier assignment and bit-loading schemes. Both sub-carrier assignment and bit-loading



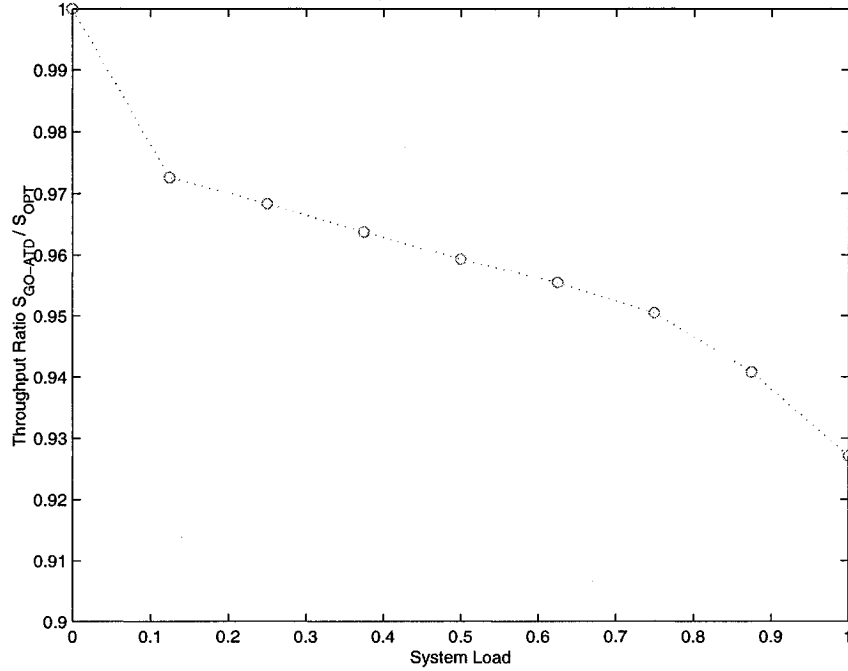


**Fig. 4.3** Throughput ratio  $S_{GO-ATD}/S_{OPT}$  at different system load.

require knowledge of the channel. If channel estimation is not accurate, the sub-carrier assignment and bit-loading computation will act according to the wrong information, and thus the system performance will be degraded. Therefore, the effect of imperfection of channel estimation has to be evaluated so that a proper margin can be added to the system design.

The focus of this study is on how the system performance changes according to the channel knowledge available to transmitters. To have a fair comparison and to remove the effect of channel knowledge on the receiver, the system model assumes perfect channel knowledge is always available at the receiver. In general, both time-domain and frequency-domain channel estimation methods exist. Time-domain estimation methods are proven to offer more accurate channel estimation [39]. The channel estimation with errors is modeled by the following equation in time domain.

$$h^{est}(n) = h(n) + \eta \quad (4.16)$$

where  $h^{est}(n)$  is the the samples of the estimated channel impulse response,  $h(n)$  is the actual channel impulse response, and  $\eta$  is a Gaussian random variable with mean zero and a predefined variance. Gaussian approximation is a good model for error with small variance [40].

As an illustration, Fig. 4.4 shows the SER degradation of the adaptive OFDMA with the optimal sub-carrier assignment scheme. The ratios of the degraded SER to the SER that should has been obtained with accurate channel information,  $SER_{deg}/SER_{aci}$ , are plotted versus the SNR for the three cases with channel error variances of -10, -20 and -30dB, where the error variances are measured with respect to the actual channel power. The performance comparison is done with a FFT size of 256, a required SER of  $10^{-2}$ , and the SUI-3 channel. The SER degradation becomes smaller as SNR increases and/or channel estimation error has smaller variances. For channel estimation error variances of -20dB or less, the corresponding SER has negligible degradation (less than 1.2). Such small increase in SER can be translated into a small degradation in SNR of less than 0.2dB, which unlikely creates change in modulation and coding level (bit-loading scheme).

#### 4.4 Chapter Summary

In this chapter, we introduced a group-optimal adaptive-tone-diversified OFDMA (GO-ATD-OFDMA) system using M-ary QAM signaling for transmitters with channel information. With the sub-carrier group structure, the complexity to compute the sub-carrier assignment is greatly reduced while the throughput performance almost matches that with the optimal sub-carrier assignment scheme. With channel information available, the GO-ATD-OFDMA scheme combines tone diversity and bit-loading techniques, and provides diversity-protected and interference-free multiple-access services. Nevertheless, like any other adaptive schemes, the performance of GO-ATD-OFDMA degrades with

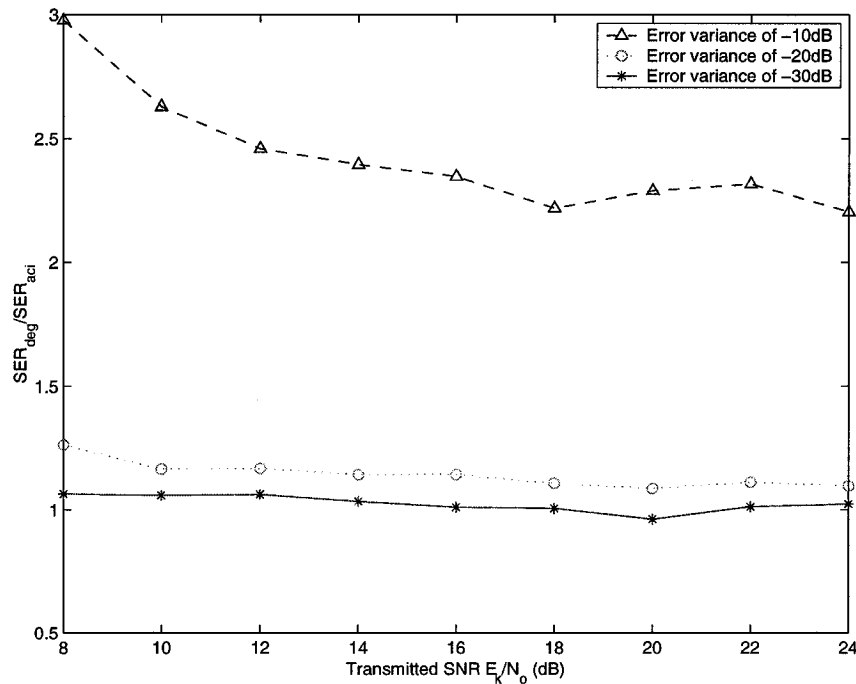


**Fig. 4.4** Degradation of SER for various error levels in channel estimation

inaccurate channel information. In the extreme case, channel estimation error might be so bad at transmitters that we can no longer assume the availability of channel information. In this case, obtaining diversity protection and maximizing spectral efficiency in a multiple-access environment is a challenging and yet interesting question. In the next chapter, based on the TC-OFDMA technique, a group-spreading OFDMA scheme will be developed with the assumption of no channel information at transmitters.

## Chapter 5

# Group-Spreading (GS) OFDMA for Transmitters without Channel Information

In this chapter, we develop a group-spreading OFDMA (GS-OFDMA) scheme under the condition that no channel information is available to transmitters. The TC-OFDMA shown in Sec. 3.3 achieves full diversity gain and no interference at the cost of low spectral utilization, which means the number of active users must be not greater than  $N/L_f$  at anytime. However, the number of active users varies in any access network, and it can be bigger than  $N/L_f$ . In such a case, the TC-OFDMA scheme cannot meet with the access demand, so a more spectral efficient scheme is needed. To increase the spectral efficiency, one easy solution is to reduce the number of sub-carriers occupied by a user. Unfortunately, this method also reduces the diversity gain of the system. To solve the conflict, we bring the idea of spreading code into the design, and propose the GS-OFDMA scheme. In Sec. 5.1, the structure of GS-OFDMA is introduced; the reason of its reduced peak-to-average power ratio (PAR) is explained; the advantages and disadvantages of the scheme is summarized, followed by a system design example

that further demonstrates how the scheme can be applied in practice. Sec. 5.2 details the signal representations of the scheme. In Sec. 5.3, maximum likelihood (ML) multi-user detection (MUD) is introduced as the optimal receiver; the tradeoff between error performance and PAR is considered as the system parameter changes; the user-loading algorithm and the system error performance are examined as well.

## 5.1 GS-OFDMA System

### 5.1.1 System Structure

The idea behind GS-OFDMA is to keep the number of sub-carriers ( $L_f$ ) in a group unchanged for full diversity gain, while allowing more than one data stream to share the same  $L_f$  sub-carriers in order to increase the spectral efficiency. Data streams sharing the same sub-carrier group are separated by distinct spreading sequences. The name of the scheme comes from the fact that spreading is done within one sub-carrier group only. Since sub-carrier groups are still orthogonal to each other, so MAI exists only among users sharing the same sub-carrier group. In the proposed scheme, data from one user is split into multiple sub-streams, and the sub-carrier group is shared with sub-streams from other users. With such a split-and-group structure, data sub-streams that come from the same user experience the same channel condition. This special property brings the benefit of simpler channel estimation. Optimal ML-MUD technique can be applied to detect signals on one sub-carrier group with relaxed complexity. More importantly, as it will be discussed in later section, due to the fact that the user sends not only one spreading sequence, but the sum of multiple spreading sequences at a time, the transmitted PAR is greatly reduced compared to traditional multi-carrier schemes. The construction of GS-OFDMA scheme can be explained by the following steps.

- Firstly, the equivalent channel order has to be estimated. The equivalent channel order is defined as the number of taps in a channel model spaced with sampling

interval. To achieve full diversity gain, a signal has to be sent through a number of sub-carriers, in which, the number of sub-carriers should not be less than the equivalent channel order. The order estimation might not and need not to be precise in a time varying channel. To insure a full diversity gain is obtained in all time, the number of sub-carriers required per user ( $L_f$ ) should satisfy Criteria 1 of Sec. 3.2. These sub-carriers are distributed evenly in the system spectrum, and form a sub-carrier group.

- Once the size of sub-carrier group ( $L_f$ ) is found, a user's data is serial to parallel converted to several sub-streams where the number of sub-streams per user ( $N_s$ ) is less than the size of sub-carrier group.
- Then each sub-stream is spread by a distinct Walsh sequence of length  $L_f$  in frequency domain, and transmitted over the members of its sub-carrier group. Different sub-streams from the same user share the same sub-carrier group with sub-streams from other users. Within a sub-carrier group, the Walsh code provides separation between sub-streams. Since sub-carrier groups are orthogonal to each other, the same Walsh code family can be recycled in every sub-carrier group.
- Because the performances of all sub-carrier groups are the same in the sense that they all have full diversity gain to combat fading, the algorithm to load users onto the system is based on the time when the user accesses the system. To minimize the interference within a sub-carrier group, users should be evenly assigned to all sub-carrier groups. In other word, when a new user comes, we assign it to the least crowded sub-carrier group.

In a sub-carrier group, as some of the sub-streams are from the same user, their data are synchronous and experience the same channel conditions. For users on different sub-carrier groups, the FFT operation with added cyclic prefix guarantees the orthogonality

between these users is maintained even when they are asynchronous and experience different channel conditions. Fig. 5.1 illustrates the sub-carrier and sub-stream assignment of a GS-OFDMA system with  $L_f$  of 4 and  $N_s$  of 2. The abbreviation ‘U#S#’ stands for ‘user # sub-stream #’.

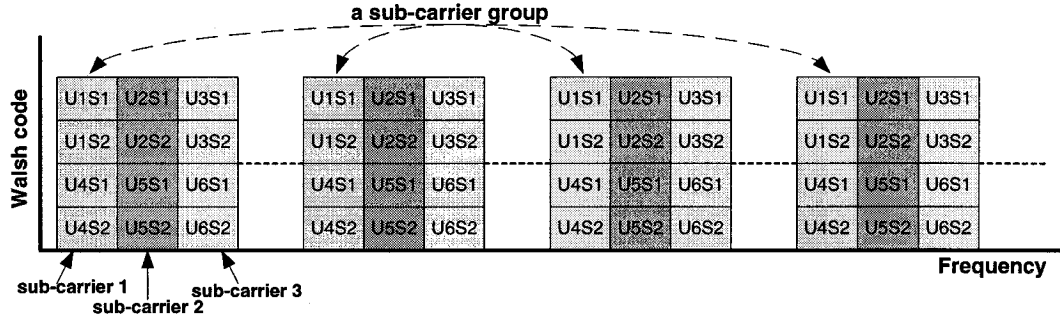


Fig. 5.1 Sub-carrier and sub-stream assignment of GS-OFDMA

An idea similar to our GS-OFDMA scheme was also developed in [28]. The main difference between their proposed GO-MC-CDMA scheme and our GS-OFDMA scheme is on the serial-to-parallel conversion of a user’s data. In other word, their GO-MC-CDMA scheme does not split user’s data into sub-streams, and hence loses the benefits of simpler channel estimation in MUD and lower transmitted PAR. Another difference is on the bandwidth of each sub-carrier. Because of the split of user’s data,  $N_s$  Walsh sequences are taken by a user, and the data rate of each sub-stream is only  $1/N_s$  of the user’s data rate. To support the same number of active users as in GO-MC-CDMA, sub-carriers in GS-OFDMA should have  $1/N_s$  of the bandwidth that GO-MC-CDMA has. A data sub-stream after the split only takes  $1/N_s$  of a user’s power, but since the symbol duration is  $N_s$  times longer at the same time, the transmitted SNR on each data sub-stream in GS-OFDMA stays the same as that in GO-MC-CDMA.

### 5.1.2 Reduced PAR

It is well known that the transmitted PAR is related to the number of tones occupied by a user in multi-carrier transmission. In both TC-OFDMA and GO-MC-CDMA schemes, if the equivalent channel order is large, it is required to occupy a large number of sub-carriers for full diversity gain. The large sub-carrier group size implies high PAR, which can be a major burden in practical implementation. Fortunately, the split-and-group structure of GS-OFDMA provides great reduction of PAR while preserving the full diversity gain.

The reason for reduced PAR relies on the fact that users send not only one spreading sequence, but the sum of several spreading sequences at a time. Fig. 5.2 illustrates the difference between using one spreading sequence and using two spreading sequences. In

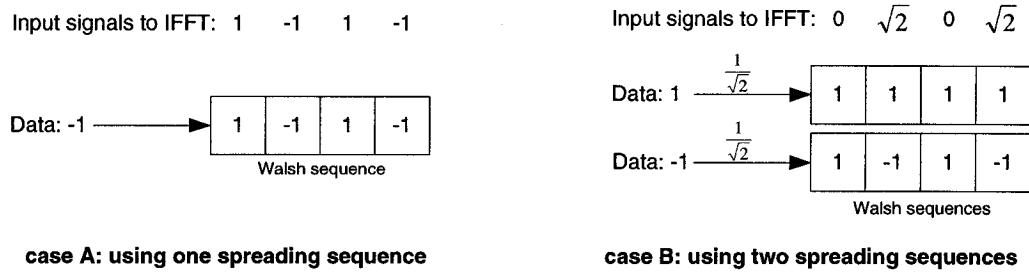


**Fig. 5.2** Difference in input signals by sending two sequences

case B, the normalized factor  $1/\sqrt{2}$  is used for the amplitude to ensure its transmitted power is the same as that in case A. One important fact we have to realize is that the normalized factor affects the peak power in the same way as it affects the average power, so no net effect on the PAR value by the normalized factor is expected. If we regard case B as a GS-OFDMA structure, the inputs to the IFFT operation are the product of two sub-stream data of a user and their assigned spreading sequences. Due to the properties of the Walsh code, half of the input signals to the IFFT are zeros and the other half will have larger amplitude no matter what the sub-stream data are. The amplitude



change can be regarded as the effect of a normalized factor. Then the inputs to the IFFT are from half of the sub-carriers only, and hence its PAR value is only half of that of traditional multi-carrier schemes. This holds for any length of Walsh sequences as long as the number of sub-streams per user,  $N_s$ , is 2.

As  $N_s$  increases, the sub-stream data combinations have an effect on the input signals to the IFFT. According to the sub-stream data and the assigned Walsh sequences, the input signals to the IFFT may or may not have zeros components. When zero components exist, the PAR value associated to this sub-stream data combination is reduced. Therefore, the average PAR value on all sub-stream data combinations is reduced in proportion to the frequency of zero input components to the IFFT.

In some special cases, the PAR value will be reduced even if there is no zero input component to the IFFT operation. For example, when  $L_f = 4$  and  $N_s = 4$ , one form of input signals to the IFFT is  $[1 \ 1 \ 1 \ -1]$  which will generate a peak power of 4 and an average power of 1. The PAR value for this input combination is 1. Actually, the input signal to the IFFT in this example has two formats only: one is all four components are with amplitude of 1 with one of them having a different sign than the rest, and the other is only one component is non-zero and with amplitude of 2. For both formats, their PAR have the same value of 1. The table below shows the reduction of PAR for different values of  $N_s$ .

**Table 5.1** Reduced PAR for different  $N_s$

$L_f$		4	8	16	32
GO-MC-CDMA		4	8	16	32
GS-OFDMA	$N_s = 2$	2	4	8	16
	$N_s = 4$	1	2	4	8
	$N_s = 8$	————	1.7071	3.4142	6.8284

In general, with the property of the Walsh code, the IFFT input signals which are generated by summing up the spreaded sub-stream data can always reduce the peak power in transmission. This demonstrates the low PAR characteristic of the GS-OFDMA

scheme.

### 5.1.3 Advantages and Disadvantage

Unlike the TC-OFDMA, the GS-OFDMA scheme achieves a high spectral efficiency while maintaining the full diversity gain. Superior to the GO-MC-CDMA, simpler channel estimations for multi-user detection is required in GS-OFDMA. In addition, the GS-OFDMA scheme has a low PAR advantage over other multi-carrier schemes.

However, due to the split-and-group structure, the FFT requirement (number of FFT points) of GS-OFDMA is high compared to the other two schemes. This requirement may be satisfied by the advance of digital signal processing techniques. Nevertheless, the low PAR advantage is not affected by the increased number of FFT points since we only need a fixed number of  $L_f$  sub-carriers to gain full diversity. Table 5.2 compares the proposed GS-OFDMA with other multi-carrier schemes in selected performance metrics.

**Table 5.2** Performance metrics comparisons of multi-carrier schemes

Type	Full diversity gain	High spectrum efficiency	Small peak-to-average power ratio	Near-far resistant
Random-hop (RH)-OFDMA	no	yes	yes	yes
MC-CDMA	yes	yes	no	no
TC-OFDMA	yes	no	no	yes
GO-MC-CDMA	yes	yes	no	no
GS-OFDMA	yes	yes	yes	no

### 5.1.4 A Design Example

To illustrate further, we consider a design example. Assuming we have the following system parameters:

- available bandwidth is 5MHz
- tolerable delay spread is 200ns

- user data rate is 64kb/s
- QPSK modulation

It is indicated in Sec. 2.5 of [15] that the period of cyclic prefix should be at least four times the tolerable delay spread to avoid inter-channel-interference (ICI) and ISI. In this example, the tolerable delay spread of 200ns means the system is pretty much interference-free if we have a cyclic prefix of 1000ns. With  $1000ns \times 5MHz = 5$ , the approximated equivalent channel order is 5. Consequently, we can design the size of sub-carrier group ( $L_f$ ) to be 8. As a result, the spreading code used for each user is Walsh sequence with length of 8. If the number of sub-streams per user ( $N_s$ ) is 2, the data rate on each sub-carrier is 32kb/s. With QPSK modulation, the required bandwidth on each sub-carrier is 16kHz. The total number of sub-carriers is  $5MHz \div 16kHz \approx 312$ , and the number of supported users is  $312 \div 8 \times 4 = 156$ . To facilitate the Fourier transform computation, we use FFT of 512 points. The data period per symbol is the inverse of the spacing between sub-carriers  $1/16kHz = 62.5\mu s$ . The loss due to the cyclic prefix is  $L_{CP} = -10 \log(62.5 \div 63.5) \approx 0.069dB$ , and the spectral efficiency of the system is  $64kb/s \times 156 \div 5MHz = 1.997b/s/Hz$ . As we can see from the above, the GS-OFDMA transmits information on all spectrum except for a small portion, and hence has a much higher frequency efficiency than the TC-OFDMA scheme does. More importantly, it realizes full diversity and can achieve superior error rate performance as shown in the later simulations.

## 5.2 Signal Model

In GS-OFDMA, users in different sub-carrier groups recycle the same Walsh code family, while users belonging to one sub-carrier group share the code family. Within one sub-carrier group, the sub-carrier allocation of a certain user is only related to the chip position of the spreading sequence. We denote  $C_{k,c,m}$  as the index of sub-carrier alloca-

tion for chip position  $c$  of user  $k$ .  $C_{k,c,m}$  is set to 1 if the  $m$ -th sub-carrier is allocated for chip position  $c$  of user  $k$ ; and is set to 0 otherwise. On sub-carrier  $m$  associated to chip position  $c$  of user  $k$ , the transmitted signals  $S_{k,n,c}$  include data from all sub-streams of user  $k$  multiplied by the chips at position  $c$  of their corresponding spreading code sequences.

$$S_{k,n,c} = \sum_{u=0}^{N_s-1} \frac{1}{\sqrt{L_f}} d_{k,n,u} \cdot a_{k,u,c} \quad (5.1)$$

where  $d_{k,n,u}$  is the data with unit energy at sub-stream  $u$  of user  $k$ , and  $a_{k,u,c}$  is the chip at position  $c$  of the spreading sequence associated to sub-stream  $u$ . The output samples from the IFFT for chip position  $c$  of user  $k$  at time instant  $n$  can then be expressed as

$$s_{k,n,c,i+L_{CPI}} = \mathcal{A}_k \sum_{m=0}^{N-1} S_{k,n,c} C_{k,c,m} e^{j2\pi m i/N}, \quad i = 0, 1, \dots, N-1 \quad (5.2)$$

At the receiver, after the cyclic prefix removal, the samples from all users can be written as

$$V_{n,i} = \sum_{k=1}^K \sum_{c=0}^{L_f-1} \sum_{l=0}^{L_t-1} \beta_{k,l} s_{k,n,c,i-l} + \eta_{n,i}, \quad i = L_{CPI}, L_{CPI} + 1, \dots, L_{CPI} + N-1 \quad (5.3)$$

Then, the FFT can be performed to extract the transmitted information-bearing symbol over each sub-carrier. The resulting signals can be shown as

$$Y_{n,m} = \sum_{k=1}^K \sum_{c=0}^{L_f-1} \mathcal{A}_k N [H_{k,m} \cdot S_{k,n,c} \cdot C_{k,c,m}] + W_{n,m} \quad (5.4)$$

For a full load, there are  $L_f/N_s$  users in one sub-carrier group. If users are sequentially assigned to sub-carrier groups, user that exists on sub-carrier  $m$  has index  $k(m, q) = 1 + \text{mod}(m, N/L_f) + (q-1)N/L_f$ , where  $q$  is the user number within a sub-carrier group that takes the value from  $[1, L_f/N_s]$ .

### 5.3 Optimal Multi-User Detection

#### 5.3.1 ML detector

ML detector is known as the optimum multi-user detector [41]. It achieves the optimum decisions by maximizing the likelihood of the received signals, or equivalently, minimizing the mean square error. Since the ML detector has to consider all possible combinations of received symbols, the computational complexity increases exponentially with the number of users, which in turn prevents it from being used widely in practice. Fortunately, in the GS-OFDMA scheme, only a small number of data sub-streams is in each sub-carrier group, which facilitates the search of the jointly optimal decisions at a low cost. Although some sub-streams in a sub-carrier group are from the same user, they can be treated as if they were from different ‘users’ but with the same channel conditions. Hence, the ML multi-user detector can be applied to the GS-OFDMA scheme to achieve optimal performance with reduced channel estimation complexity. The jointly optimum decision searching problem can be formulated as minimizing the following expression.

$$\sum_{i=0}^{L_f-1} \left\| Y_{n,m_i} - \sum_{k=1}^K \sum_{c=0}^{L_f-1} \mathcal{A}_k N \left[ H_{k,m_i} \hat{S}_{k,n,c} C_{k,c,m_i} \right] \right\|^2 \quad (5.5)$$

where  $m_i = m_o + i \cdot N/L_f$  and  $\hat{S}_{k,n,c}$  is a guess of the transmitted  $S_{k,n,c}$ .

To see how the ML detector performs in the GS-OFDMA scheme, Fig. 5.3 shows the SER comparison between the GS-OFDMA, GO-MC-CDMA and single-user RAKE receiver. A 3-tap Rayleigh fading channel model with equal-power paths is used, and the spreading factor employed is 4. Assuming there are 64 users with QPSK modulation and  $N_s$  is chosen to be 2, 128-point FFT is used for GS-OFDMA, while 64-point FFT is applied to GO-MC-CDMA. The result shows the performance gap between the GS-OFDMA and the theoretical single-user Rake receiver is about 1.5dB except in the high SNR region. The gaps to both single-user Rake receiver and GO-MC-CDMA become

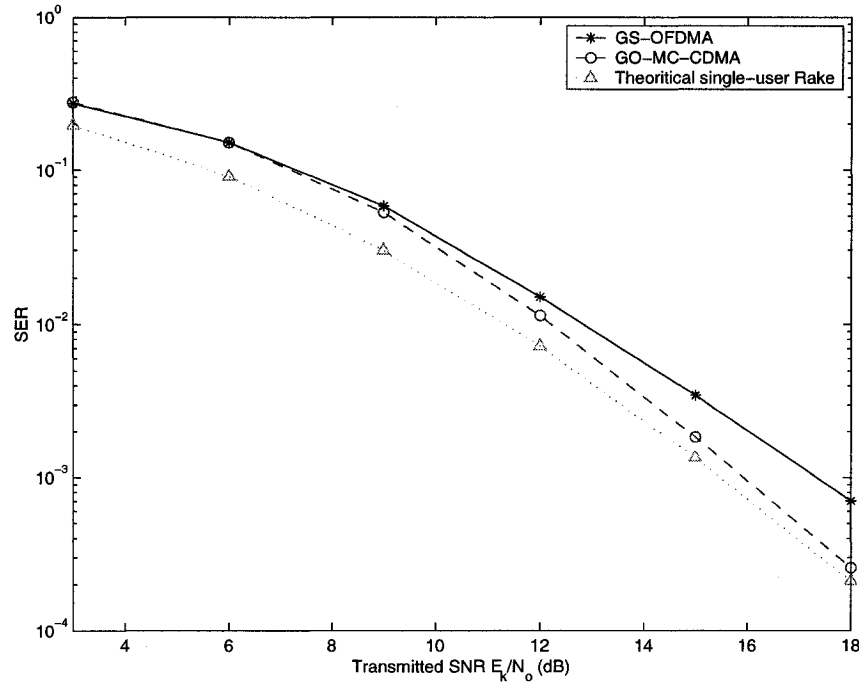


Fig. 5.3 SER comparison between GS-OFDMA and GO-MC-CDMA

wider when the SNR is high.

The reason for performance discrepancy between GO-MC-CDMA and GS-OFDMA in high SNR lies in the cross-correlation matrix  $R$  of the systems. When the value of SNR is high, noise is no longer the dominant factor in deciding the performance, but the cross-correlation matrix  $R$  determines the performance of multi-user detection. The cross-correlation matrix  $R$  includes the effect of channels. As some ‘users’ in GS-OFDMA have identical channel condition, their corresponding elements in  $R$  are more correlated. This makes the interference worse than that of GO-MC-CDMA, which has less correlation between elements of its  $R$  matrix since channel conditions are independently generated for different users.

### 5.3.2 Effect of $N_s$

The factor to decide how many ‘users’ have identical channel conditions is the number of sub-streams per user,  $N_s$ . As  $N_s$  affects the cross-correlation matrix  $R$ , it has an

impact on the performance of MUD. This observation is confirmed by the simulation results shown in Fig. 5.4. The SER performance is compared for GS-OFDMA with

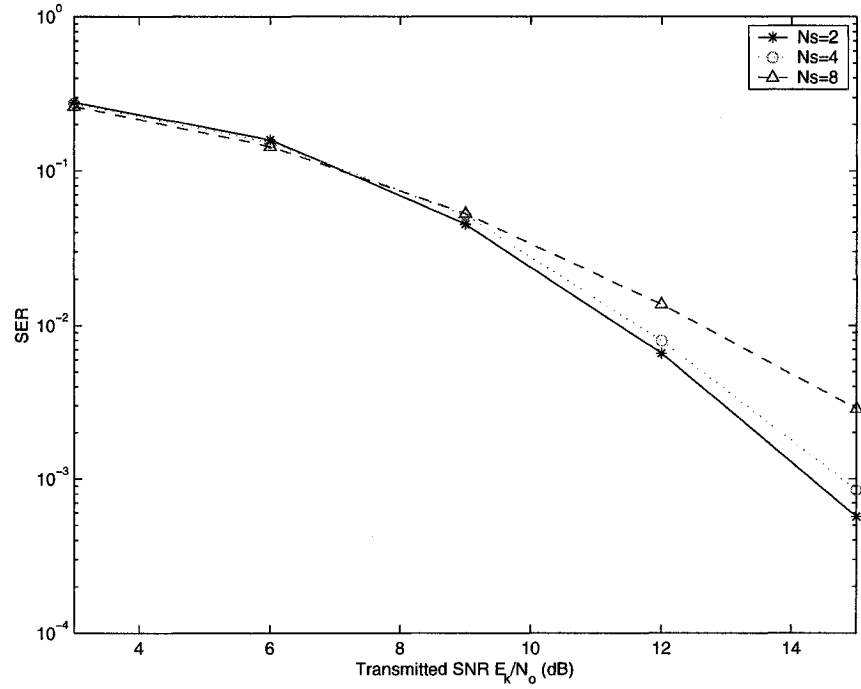


**Fig. 5.4** The effect of  $N_s$  on the error rate performance

three different values of  $N_s$ . A 6-tap Rayleigh fading channel model with exponential decaying power profile (i.e., 0, -2.6, -5.2, -7.8, -10.4, -13.0dB) is used.  $L_f$  is chosen to be 8, and  $N_s$  equals to 2, 4 and 8 respectively. As we can see, as  $N_s$  becomes larger, the system performance becomes worse. On the other hand, larger  $N_s$  implies lower PAR. Therefore, when designing the value of  $N_s$ , the trade-off between PAR minimization and error rate performance should be considered.

### 5.3.3 Performance of User-Loading Algorithm

So far, the system performance has been shown for the case of full system load. To study the behaviour of our user-loading algorithm, Fig. 5.5 compares the system SER to the theoretical single-user Rake receiver SER at different loading values. The simulation is performed with  $E_s/N_o$  of 12dB,  $L_f$  of 8,  $N_s$  of 2, and QPSK modulation in a 8-tap

Rayleigh fading channel model with exponential decaying power profile (i.e., 0, -1.7, -3.5, -5.2, -6.9, -8.7, -10.4, -12.2dB). The system SER shows little degradation as compared to the optimal case at all loading levels.

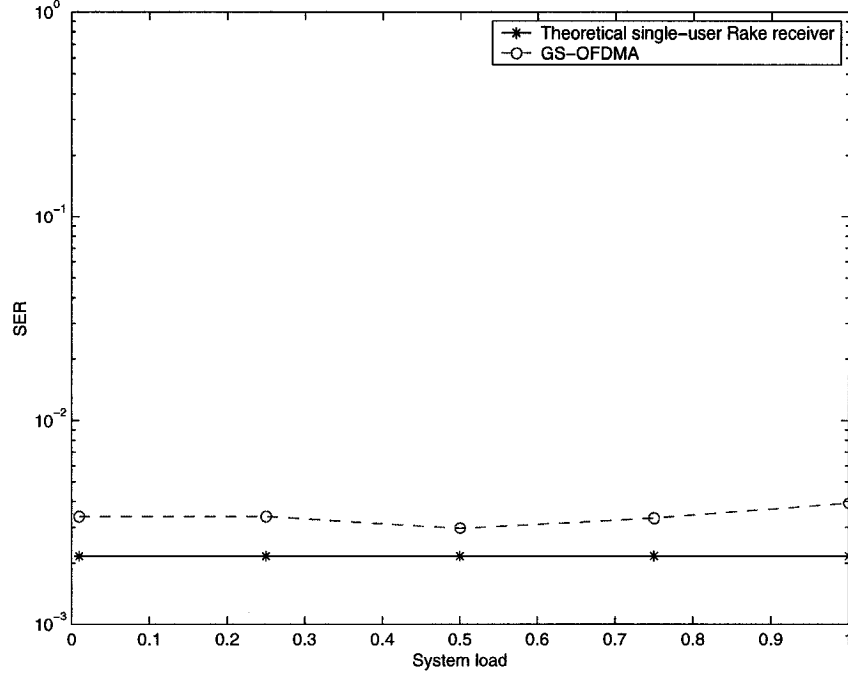


Fig. 5.5 SER performance of GS-OFDMA at different system load

#### 5.3.4 SER Performance Comparisons

At last, the practical channel model, SUI-3, is chosen to reveal the performance gain of GS-OFDMA over other traditional multi-carrier systems. With a sampling frequency of 5MHz, the value of  $L_f$  is selected to be 8 to have full diversity gain. With  $N_s$  of 2, QPSK modulation, and 512-point FFT implemented, the GS-OFDMA system parameters match those in the design example in Sec.5.1.4. The matched filter receiver is assumed on MC-CDMA for the simplicity of structure, while multi-user detection is used on GO-MC-CDMA and GS-OFDMA. Without any data split, 256-point FFT are used in RH-OFDMA, MC-CDMA, TC-OFDMA and GO-MC-CDMA. It is also assumed that cooperative hopping patterns among all users are implemented in RH-OFDMA. Fig. 5.6



shows the performance comparison of SER. The TC-OFDMA system only supports  $1/8$  of the number of users that other systems support, and its curve serves as the lower bound. The error rate performance of GS-OFDMA is slightly inferior to the GO-MC-

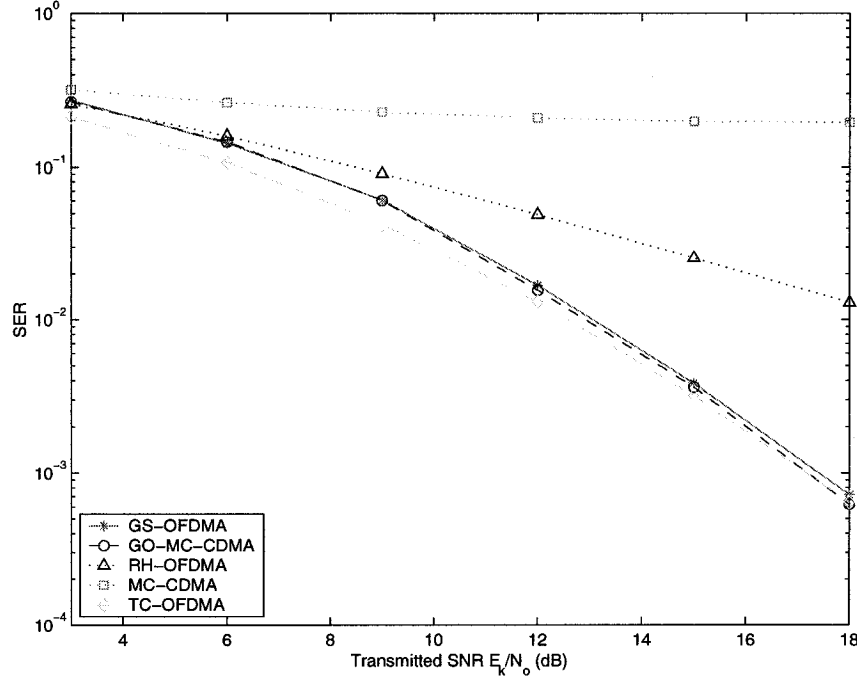


Fig. 5.6 SER comparison of different multi-carrier systems

CDMA scheme only. As SNR improves, the gap between GS-OFDMA and GO-MC-CDMA becomes wider. However, the curve of GS-OFDMA converges to the optimal curve. This contradicts the previous observation in Sec. 5.3.1. One possible reason that explains the contradiction is the spreading factor. In previous observations, we chose  $L_f = 4$  and  $N_s = 2$ , while we have  $L_f = 8$  and  $N_s = 2$  in this example. As we can see, the number of sub-streams with extra correlation stays the same. But, with larger  $L_f$ , the randomness between the two sub-streams from the same user increases, and hence the effect of extra correlation is reduced. Therefore, even if the error performance of GS-OFDMA is still worse than that of GO-MC-CDMA, a large  $L_f$  can help close the gap to the optimum case in high SNR region. Nevertheless, a large  $L_f$  also increases the complexity of MUD.

## **5.4 Chapter Summary**

In this chapter, we proposed a GS-OFDMA scheme that does not require channel information at transmitters. The scheme inherits TC-OFDMA's full diversity gain, and achieves high spectral efficiency. With its split-and-group structure and the property of Walsh code, the transmitted PAR of GS-OFDMA is greatly reduced. In the error rate performance evaluation, the GS-OFDMA scheme outperforms both RH-OFDMA and MC-CDMA because of its ability to achieve full diversity gain and interference suppression. The limited interference exists only within a small group of users, and hence the optimal ML multi-user detection can be applied to mitigate the effect of interference. With its error rate performance nearly matching that of the GO-MC-CDMA scheme, GS-OFDMA provides advantages of low transmitted PAR and simpler channel estimation over MUD. Overall, GS-OFDMA with simple structure is an attractive multiple-access scheme that provides high spectral efficiency and good error performance in scenarios where no channel information can be made available to transmitters.

# Chapter 6

## Conclusions

This chapter summarizes the key research findings, and recommends some topics for future studies.

### 6.1 Summary of Research Findings

The first chapter introduced OFDMA for broadband wireless communications, and highlighted the importance of diversity in OFDMA. Losses of data could be caused by the occurrence of deep fades in frequency-selective fading channels. Diversity techniques can be applied to OFDMA to improve the system performance. The objective of developing cost-effective diversity techniques for OFDMA was stated at the end of the chapter.

To understand the cause of frequency-selective fading, the multipath property of wireless channels was firstly reviewed in Chapter 2. Then, as a solution to combat fading, a ZCZ-CDMA scheme was shown to achieve both diversity-protected and interference-free transmission due to the perfect auto-correlation and cross-correlation property of the ZCZ code. However, the perfect correlation property sacrifices the family size of the ZCZ code, and hence limits the implementation of the ZCZ-CDMA scheme. OFDMA was introduced as a cyclic non-spreading CDMA scheme, where the orthogonality among users is maintained by the design of the cyclic prefix. Nevertheless, transmissions in

OFDMA require diversity protection. It was found from the literature review that a group-orthogonal (GO) MC-CDMA scheme, which is based on the scheme of OFDMA, achieves diversity gain. However, the issue of high PAR induced by using multiple sub-carriers may cause the concern of power efficiency.

To develop diversity technique for OFDMA, its frequency-domain diversity characteristic was examined in Chapter 3. It was mathematically proven that the full diversity gain as obtained by a time-domain CDMA Rake receiver can be achieved by using  $L_f$  sub-carriers, as long as  $L_f$  is not less than the number of taps of the transformed channel model,  $L_t$ . The established diversity equivalence also suggests a systematic sub-carrier assignment method for OFDMA to achieve the full diversity gain. Specifically, to have the exact full diversity gain while minimizing the degradation of spectral efficiency, the selection of  $L_f$  must be the minimum power of 2 not less than  $L_t$ . These  $L_f$  sub-carriers are evenly distributed in the system spectrum, and form a sub-carrier group. With the formation of sub-carrier groups, a tone-selective (TS) technique requiring channel information at transmitters and a tone-combined (TC) technique without the need of channel information at transmitters were discussed. It has been shown that the TC-OFDMA scheme reaches the single-user Rake receiver's performance by using a sub-carrier group for transmissions, while the TS-OFDMA surpasses the single-user Rake receiver by selecting the most suitable sub-carrier within a group for transmissions. The closed-form BER expressions, which conforms with the simulation results, were derived for the two schemes over multipath frequency-selective Rayleigh fading channels. Although the two schemes achieve diversity gain, the system spectral efficiency is decreased due to the assignment of one sub-carrier group per user.

In Chapter 4, to increase the spectral efficiency in scenarios where channel information is available at transmitters, we proposed the group-optimal adaptive-tone-diversity (GO-ATD) OFDMA scheme that combines the TS technique with the adaptive M-ary QAM signaling. We presented the structure of the GO-ATD-OFDMA and showed how

it realized the optimal sub-carrier assignment within each sub-carrier group. Due to the sub-carrier group structure, the complexity to compute our sub-carrier assignment is  $\mathcal{O}(N \cdot L_f)$ , while the complexity to compute the optimal sub-carrier assignment is  $\mathcal{O}(N^2)$ . On the other hand, the throughput comparisons showed the proposed scheme not only is more spectral efficient than the RH-OFDMA, but also can provide a comparable performance to the optimal sub-carrier assignment scheme. For instance, the throughput of the GO-ATD-OFDMA can achieve 92.7% of that of the optimal sub-carrier assignment scheme at the full load, while its computational complexity is only  $\frac{L_f}{N} = \frac{1}{32}$  over the SUI-3 channel. The great reduction in computational complexity makes a quick sub-carrier re-assignment of GO-ATD-OFDMA possible. Nevertheless, the good performance of GO-ATD-OFDMA relies on the accuracy of channel estimation. Simulations to measure the effect of erroneous channel information showed the system performance has negligible degradation for error with small variance, i.e., -30dB.

Under the condition of no reliable channel estimation, the group-spreading (GS) OFDMA scheme that does not require channel information at transmitters was developed in Chapter 5. By incorporating spreading with the TC technique, the GS-OFDMA scheme achieves not only full diversity gain, but also a high spectral efficiency. Compared to other traditional multi-carrier schemes, the transmitted PAR of GS-OFDMA is greatly reduced due to its split-and-group structure and the property of the Walsh code. The PAR value will be reduced further as the number of sub-streams per user,  $N_s$ , increases. On the other hand, as  $N_s$  increases, the MUD will become more difficult due to the more correlated elements in the cross-correlation matrix  $R$ . Hence, the selection of  $N_s$  has to balance between PAR minimization and error rate performance. In the performance evaluation, the investigation of the SER at different system loads showed little degradation as compared to the case of a single-user Rake receiver; the comparison with other traditional multi-carrier systems demonstrated a superior performance of the GS-OFDMA scheme to both the RH-OFDMA and the MC-CDMA schemes, and a nearly

matching performance to the GO-MC-CDMA scheme while providing the advantages of lower transmitted PAR and simpler channel estimation for MUD.

## 6.2 Suggestions for Future Research

The OFDMA is a promising scheme for future generation broadband wireless networks. Although this thesis has addressed some topics, there are still relevant and meaningful works remaining untouched. Some suggestions for future research in the context of this thesis are listed as follows.

- Current work studied two cases depending on whether or not the channel information is known to transmitters. In practice, even when the channel information is known to transmitters, the channel can be time-varying and its information needs to be updated. The update rate might be once per frame or once several frames. This brings us an interesting question, which is what to use between two updates. One can use the result from the last update, implying that the channel is time-invariant till the next update, or one can do some channel prediction. Since this thesis reveals that by knowing accurately the channel information, the resource allocation could be done much better. One can expect that the channel prediction could help the resource allocation and thus the system performance. Therefore, to study the OFDMA with channel prediction in a time-varying channel would be an interesting topic.
- This thesis established a simple framework of an OFDMA system and considered single-cell only. How the OFDMA scheme works in a multi-cell system could be another interesting topic. In the multi-cell system, due to the fact that many cells are sharing the same frequency band, the inter-cell interference can be a major factor limiting the system performance. How to suppress both inter-cell and intra-cell interference, while still achieving full diversity gain and a high frequency re-use

ratio is an interesting yet challenging research topic. To effectively enhance the spectral utilization in a multi-cell, multi-user, and multipath environment, it is worth investigating how we can develop from the proposed single-cell techniques an adaptive resource allocation scheme that combines bit-loading, power control, sub-carrier assignment and code implementation.

- This thesis considered the OFDMA scheme in single-input and single-output system. Recently, there has been a growing interest in multiple-input multiple-output (MIMO) related systems. With multiple transmitted and received antennas, multiple parallel links (one link might be correlated with another) can be established. The signal over each link can be OFDM modulated. Hence, multiple links provide more alternatives in the selection of the tones for transmissions, and also bring us the challenge on how to avoid the interference from one link to another if they are correlated. Moreover, based on the frequency-domain diversity characteristics, an interesting research topic will be the design of a space-time-frequency code that not only exploits the full multipath diversity but also maximizes the system throughput.

Overall, the OFDMA is a very appealing scheme and it has the great potential for wireless applications over frequency-selective fading channels.

## Appendix A

### BER Derivation of TS-OFDMA

The closed-form BER expression for TS-OFDMA is derived as follows.

$$\begin{aligned}
 P_b &= \int_0^\infty P_b(e|\gamma_{b,k}) p(\gamma_{b,k}) d\gamma_{b,k} \\
 &= \frac{L_f}{\Gamma_b} \int_0^\infty P_b(e|\gamma_{b,k}) e^{-\gamma_{b,k}/\Gamma_b} (1 - e^{-\gamma_{b,k}/\Gamma_b})^{L_f-1} d\gamma_{b,k} \\
 &= \frac{L_f}{\Gamma_b} \frac{1}{\log_2(I \cdot J)} \int_0^\infty \left( \sum_{a=1}^{\log_2 I} P_I(a) + \sum_{b=1}^{\log_2 J} P_J(b) \right) \\
 &\quad \cdot e^{-\gamma_{b,k}/\Gamma_b} (1 - e^{-\gamma_{b,k}/\Gamma_b})^{L_f-1} d\gamma_{b,k} \tag{A.1}
 \end{aligned}$$

We only need to solve  $\int_0^\infty \sum_{a=1}^{\log_2 I} P_I(a) e^{-\gamma_{b,k}/\Gamma_b} (1 - e^{-\gamma_{b,k}/\Gamma_b})^{L_f-1} d\gamma_{b,k}$  since  $P_I(a)$  and  $P_J(b)$  are symmetric.

$$\begin{aligned}
 &\int_0^\infty \sum_{a=1}^{\log_2 I} P_I(a) e^{-\gamma_{b,k}/\Gamma_b} (1 - e^{-\gamma_{b,k}/\Gamma_b})^{L_f-1} d\gamma_{b,k} \\
 &= \sum_{a=1}^{\log_2 I} \int_0^\infty P_I(a) e^{-\gamma_{b,k}/\Gamma_b} (1 - e^{-\gamma_{b,k}/\Gamma_b})^{L_f-1} d\gamma_{b,k} \\
 &= \sum_{a=1}^{\log_2 I} \frac{1}{I} \sum_{c=0}^{(1-2^{-a})I-1} (-1)^{\lfloor \frac{c \cdot 2^{a-1}}{I} \rfloor} \left[ 2^{a-1} - \left\lfloor \frac{c \cdot 2^{a-1}}{I} + \frac{1}{2} \right\rfloor \right] \\
 &\quad \cdot \int_0^\infty \text{erfc} \left[ (2c+1) \sqrt{\frac{3 \log_2(I \cdot J) \gamma_{b,k}}{I^2 + J^2 - 2}} \right] e^{-\gamma_{b,k}/\Gamma_b} (1 - e^{-\gamma_{b,k}/\Gamma_b})^{L_f-1} d\gamma_{b,k} \tag{A.2}
 \end{aligned}$$



After using the Binomial Theorem,  $(a + b)^n = \sum_{i=0}^n \binom{n}{i} a^i b^{(n-i)}$ , the integral term of Eq. (A.2) becomes

$$\begin{aligned} & \int_0^\infty \operatorname{erfc} \left[ (2c+1) \sqrt{\frac{3 \log_2(I \cdot J) \gamma_{b,k}}{I^2 + J^2 - 2}} \right] \sum_{i=0}^{L_f-1} \binom{L_f-1}{i} (-1)^i e^{-\frac{\gamma_{b,k}(i+1)}{\Gamma_b}} d\gamma_{b,k} \\ &= \sum_{i=0}^{L_f-1} \binom{L_f-1}{i} (-1)^i \int_0^\infty \operatorname{erfc} \left[ (2c+1) \sqrt{\frac{3 \log_2(I \cdot J) \gamma_{b,k}}{I^2 + J^2 - 2}} \right] e^{-\frac{\gamma_{b,k}(i+1)}{\Gamma_b}} d\gamma_{b,k} \quad (\text{A.3}) \end{aligned}$$

To solve the integral of Eq. (A.3), we need to find a solution for the general form  $\int_0^\infty \operatorname{erfc}(a\sqrt{\gamma_{b,k}}) e^{-b\gamma_{b,k}} d\gamma_{b,k}$ . By using the identity  $\int_0^\infty \operatorname{erfc}(\sqrt{x}) e^{-ax} dx = \frac{1}{a} [1 - \frac{1}{\sqrt{1+a}}]$  [35], it can be shown that

$$\int_0^\infty \operatorname{erfc}(a\sqrt{\gamma_{b,k}}) e^{-b\gamma_{b,k}} d\gamma_{b,k} = \frac{1}{b} \left[ 1 - \frac{1}{\sqrt{1+b/a^2}} \right] \quad (\text{A.4})$$

Substitute  $a = (2c+1) \sqrt{\frac{3 \log_2(IJ) \gamma_{b,k}}{I^2 + J^2 - 2}}$  and  $b = \frac{i+1}{\Gamma_b}$  into Eq. (A.4), we solve the integral of Eq. (A.3).

$$\begin{aligned} & \int_0^\infty \operatorname{erfc} \left[ (2c+1) \sqrt{\frac{3 \log_2(I \cdot J) \gamma_{b,k}}{I^2 + J^2 - 2}} \right] e^{-\frac{\gamma_{b,k}(i+1)}{\Gamma_b}} d\gamma_{b,k} \\ &= \frac{\Gamma_b}{i+1} \left[ 1 - (2c+1) \sqrt{\frac{\Gamma_b \cdot 3 \log_2(IJ)}{\Gamma_b(2c+1)^2 \cdot 3 \log_2(IJ) + (i+1)(I^2 + J^2 - 2)}} \right] \quad (\text{A.5}) \end{aligned}$$

After substituting Eq. (A.5) into Eq. (A.3), we find a closed form expression for Eq. (A.2).

$$\begin{aligned}
& \int_0^\infty \sum_{a=1}^{\log_2 I} P_I(a) e^{-\gamma_{b,k}/\Gamma_b} (1 - e^{-\gamma_{b,k}/\Gamma_b})^{L_f-1} d\gamma_{b,k} \\
&= \sum_{a=1}^{\log_2 I} \frac{1}{I} \sum_{c=0}^{(1-2^{-a})I-1} (-1)^{\lfloor \frac{c \cdot 2^{a-1}}{I} \rfloor} \left[ 2^{a-1} - \left\lfloor \frac{c \cdot 2^{a-1}}{I} + \frac{1}{2} \right\rfloor \right] \sum_{i=0}^{L_f-1} \binom{L_f-1}{i} (-1)^i \cdot \\
&\quad \cdot \frac{\Gamma_b}{i+1} \left[ 1 - (2c+1) \sqrt{\frac{\Gamma_b \cdot 3 \log_2(IJ)}{\Gamma_b(2c+1)^2 \cdot 3 \log_2(IJ) + (i+1)(I^2 + J^2 - 2)}} \right] \\
&= \frac{\Gamma_b}{I} \sum_{a=1}^{\log_2 I} \sum_{c=0}^{(1-2^{-a})I-1} \Theta(c, a, I) \sum_{i=0}^{L_f-1} \binom{L_f-1}{i} \frac{(-1)^i}{i+1} \cdot \\
&\quad \cdot \left[ 1 - \sqrt{\frac{\aleph(c, I, J)}{\aleph(c, I, J) + (i+1)(I^2 + J^2 - 2)}} \right] \tag{A.6}
\end{aligned}$$

where  $\Theta(a, b, c) = (-1)^{\lfloor \frac{a \cdot 2^{b-1}}{c} \rfloor} \left[ 2^{b-1} - \left\lfloor \frac{a \cdot 2^{b-1}}{c} + \frac{1}{2} \right\rfloor \right]$  and  $\aleph(a, b, c) = 3\Gamma_b(2a+1)^2 \log_2(bc)$ .

The following manipulations simplify the expression in Eq. (A.6) further.

$$\begin{aligned}
& \sum_{i=0}^{L_f-1} \binom{L_f-1}{i} \frac{(-1)^i}{i+1} \left[ 1 - \sqrt{\frac{\aleph(c, I, J)}{\aleph(c, I, J) + (i+1)(I^2 + J^2 - 2)}} \right] \\
&= \sum_{i=0}^{L_f-1} \frac{L_f (L_f-1)! (-1)^i}{L_f i! (L_f-1-i)! (i+1)} \left[ 1 - \sqrt{\frac{\aleph(c, I, J)}{\aleph(c, I, J) + (i+1)(I^2 + J^2 - 2)}} \right] \\
&= \sum_{i=0}^{L_f-1} \frac{L_f! (-1)^i}{L_f (L_f-1-i)! (i+1)!} \left[ 1 - \sqrt{\frac{\aleph(c, I, J)}{\aleph(c, I, J) + (i+1)(I^2 + J^2 - 2)}} \right] \\
&= \frac{1}{L_f} \sum_{i=1}^{L_f} \binom{L_f}{i} (-1)^{i-1} \left[ 1 - \sqrt{\frac{\aleph(c, I, J)}{\aleph(c, I, J) + i(I^2 + J^2 - 2)}} \right] \\
&= \frac{1}{L_f} \left[ \sum_{i=1}^{L_f} \binom{L_f}{i} (-1)^{i-1} + \sum_{i=1}^{L_f} \binom{L_f}{i} (-1)^i \sqrt{\frac{\aleph(c, I, J)}{\aleph(c, I, J) + i(I^2 + J^2 - 2)}} \right] \\
&= \frac{1}{L_f} \left[ 1 + \sum_{i=1}^{L_f} \binom{L_f}{i} (-1)^i \sqrt{\frac{\aleph(c, I, J)}{\aleph(c, I, J) + i(I^2 + J^2 - 2)}} \right] \\
&= \frac{1}{L_f} \sum_{i=0}^{L_f} \binom{L_f}{i} (-1)^i \sqrt{\frac{\aleph(c, I, J)}{\aleph(c, I, J) + i(I^2 + J^2 - 2)}} \tag{A.7}
\end{aligned}$$

Finally, combining Eq. (A.1), Eq. (A.6) and Eq. (A.7) generates a closed-form expression for the BER of TS-OFDMA scheme.

$$\begin{aligned}
P_b &= \frac{1}{\log_2(I \cdot J)} \left[ \sum_{a=1}^{\log_2 I} \frac{1}{I} \sum_{c=0}^{(1-2^{-a})I-1} \Theta(c, a, I) \sum_{i=0}^{L_f} \binom{L_f}{i} (-1)^i \cdot \right. \\
&\quad \cdot \sqrt{\frac{\aleph(c, I, J)}{\aleph(c, I, J) + i(I^2 + J^2 - 2)}} + \sum_{b=1}^{\log_2 J} \frac{1}{J} \sum_{c=0}^{(1-2^{-b})J-1} \Theta(c, b, J) \cdot \\
&\quad \cdot \sum_{i=0}^{L_f} \binom{L_f}{i} (-1)^i \sqrt{\frac{\aleph(c, I, J)}{\aleph(c, I, J) + i(I^2 + J^2 - 2)}} \left. \right] \\
&= \frac{1}{\log_2(I \cdot J)} \left[ \sum_{a=1}^{\log_2 I} \frac{1}{I} \sum_{c=0}^{(1-2^{-a})I-1} \Theta(c, a, I) \cdot \Omega(c, I, J) + \right. \\
&\quad \left. + \sum_{b=1}^{\log_2 J} \frac{1}{J} \sum_{c=0}^{(1-2^{-b})J-1} \Theta(c, b, J) \cdot \Omega(c, I, J) \right] \tag{A.8}
\end{aligned}$$

where  $\Omega(a, b, c) = \sum_{i=0}^{L_f} \binom{L_f}{i} \cdot (-1)^i \sqrt{\frac{\aleph(a, b, c)}{\aleph(a, b, c) + i(b^2 + c^2 - 2)}}$ .

## References

- [1] I. Koffman and V. Roman, "Broadband wireless access solutions based on OFDM access in IEEE 802.16," *IEEE Commun. Mag.*, pp. 96–103, Apr. 2002.
- [2] J. Chuang and N. Sollenberger, "Beyond 3G: wideband wireless data access based on OFDM and dynamic packet assignment," *IEEE Commun. Mag.*, vol. 39, pp. 78–87, Jul. 2000.
- [3] J. A. C. Bingham, "Multicarrier modulation for data transmission: an idea whose time has come," *IEEE Commun. Mag.*, pp. 5–14, May 1990.
- [4] L. Tomba and W. A. Krzymien, "Reverse link performance of a coded OFDM/SFH-CDMA transmission scheme," *Signal Processing Advances in Wireless Communications, 1997 First IEEE Signal Processing Workshop on*, pp. 241–244, April 1997.
- [5] K. L. Baum and N. S. Nadgauda, "A comparison of differential and coherent reception for a coded OFDM system in a low C/I environment," *Global Telecommunications Conference, 1997. GLOBECOM '97., IEEE*, vol. 1, pp. 300–304, Nov. 1997.
- [6] T. S. Rappaport, *Wireless Communications: Principles and Practice*. USA: Prentice Hall PTR, first ed., 1996.
- [7] W. Ye and A. Haimovich, "Performance of cellular cdma with cell site antenna arrays, rayleigh fading, and power control error," *IEEE Trans. Commun.*, vol. 48, pp. 1151 – 1159, July 2000.
- [8] J. Zhang, E. Chong, and I. Kontoyiannis, "Unified spatial diversity combining and power allocation for cdma systems in multiple time-scale fading channels," *IEEE J. Select. Areas Commun.*, vol. 19, pp. 1276 – 1288, July 2001.
- [9] N. Suehiro, "A signal design without co-channel interference for approximately synchronized CDMA systems," *IEEE J. Select. Areas Commun.*, vol. JSAC-12, pp. 837–841, June 1994.
- [10] P. Z. Fan, N. Suehiro, N. Kuroyanagi, and X. Deng, "Class of binary sequences with zero correlation zone," *IEE Electronics Letters*, vol. 36, pp. 777–779, May 1999.

- [11] Y. L. Xu, J. Weng, and T. Le-Ngoc, "DS-CDMA for uplink low data rate transmission in multi-beam satellite communications: radio capacity performance," *IEEE Canadian Conf. on Elec. and Comp. Engineering*, vol. 3, pp. 1523–1526, May 2003.
- [12] X. Deng and P. Fan, "Spreading sequence sets with zero correlation zone," *IEE Electronics Letters*, vol. 36, pp. 993–994, May 2000.
- [13] J. S. Cha, S. Kameda, M. Yokoyama, H. Nakase, K. Masu, and K. Tsubouchi, "New binary sequences with zero-correlation duration for approximately synchronised CDMA," *IEE Electronics Letters*, vol. 36, pp. 991–993, May 2000.
- [14] X. H. Tang, P. Z. Fan, and S. Matsufuji, "Lower bounds on correlation of spreading sequence set with low of zero correlation zone," *Electronic Letters*, vol. 36, pp. 551–552, Mar. 2000.
- [15] R. V. Nee and R. Prasad, *OFDM for Wireless Multimedia Communications*. Universal Personal Communications, The Artech House, 2000.
- [16] J. Weng, T. Le-Ngoc, and Y. L. Xu, "ZCZ-CDMA and OFDMA using M-QAM for broadband wireless communications," *J. Wireless Commun. and Mobile Comput.*, vol. 4, pp. 427–438, June 2004.
- [17] J. S. Chow, J. C. Tu, and J. M. Cioffi, "A discrete multitone transceiver system for HDSL applications," *IEEE J. Select. Areas Commun.*, vol. 9, pp. 895–908, Aug. 1991.
- [18] N. Kong, "Average signal-to-interference-plus-noise ratio of a generalized optimum selection combiner for non-identical independent Rayleigh fading channels in the presence of co-channel interference," *Communications, IEEE International Conference on*, vol. 4, pp. 990–994, June 2001.
- [19] Y. Doi, T. Ohgane, and Y. Karasawa, "Down-link performance of interference canceller combining path pre-selecting adaptive array and cascaded equalizer," *IEEE Trans. Vehi. Tech.*, vol. 3, pp. 2512–2516, May 1998.
- [20] P. A. Ranta, A. Lappetelainen, and Z. C. Honkasalo, "Interference cancellation by joint detection in random frequency hopping TDMA networks," *Universal Personal Communications, 1996 5th IEEE International Conference on*, vol. 1, pp. 428–432, Sept. 1996.
- [21] R. D. Gaudenzi, C. Elia, and R. Viola, "Bandlimited quasi-synchronous cdma: A novel satellite access technique for mobile and personal communication systems," *IEEE J. Select. Areas Commun.*, vol. 10, pp. 328–343, Feb. 1992.
- [22] X. D. Lin and K. H. Chang, "Optimal PN sequence design for quasisynchronous CDMA communication systems," *IEEE Trans. Commun.*, vol. 45, pp. 221–226, Feb. 1997.

- [23] S. R. Park, I. Song, S. Yoon, and J. Lee, "A new polyphase sequence with perfect even and good odd cross-correlation functions for DS/CDMA systems," *IEEE Trans. Vehi. Tech.*, vol. 51, no. 5, 2002.
- [24] T. Seki, M. Itami, H. Ohta, and K. Itoh, "A study of OFDM system applying frequency diversity," *Personal, Indoor and Mobile Radio Communications, 2000, PIMRC 2000. The 11th IEEE International Symposium on*, vol. 2, pp. 1385–1389, Sept. 2000.
- [25] S. Zhou and G. B. Giannakis, "Frequency-hopped generalized MC-CDMA for multipath and interference suppression," in *Proc. of MILCOM Conf.*, pp. 937–942, Oct. 2000.
- [26] G. B. Giannakis, Z. Wang, A. Scaglione, and S. Barbarossa, "AMOUR-Generalized Multicarrier Transceivers for Blind CDMA Regardless of Multipath," *IEEE Trans. Commun.*, vol. 48, pp. 2064–2076, Dec. 2000.
- [27] G. Leus, S. Zhou, and G. B. Giannakis, "Orthogonal Multiple Access Over Time- and Frequency-Selective Channels," *IEEE Trans. Info. Theory*, vol. 49, pp. 1942–1950, Aug. 2003.
- [28] X. Cai, S. Zhou, and G. B. Giannakis, "Group-Orthogonal Multicarrier CDMA," *IEEE Trans. Commun.*, vol. 52, pp. 90–99, Jan. 2004.
- [29] J. Weng and T. Le-Ngoc, "Rake receiver using blind adaptive minimum output energy detection for DS/CDMA over multipath fading channels," *IEE Proc. Commun.*, vol. 148, pp. 385–392, Dec. 2001.
- [30] T. Kaitz, M. Goldhammer, N. Chayat, and V. Yanover, "Uplink OFDMA for the 256 FFT mode," in *IEEE C802.16a-02/37*, IEEE, Mar. 2002.
- [31] S. Hara and R. Prasad, "Design and performance of multicarrier CDMA system in frequency-selective rayleigh fading channels," *IEEE Trans. Vehi. Tech.*, vol. VT-48, pp. 1584–1595, Sept. 1999.
- [32] J. G. Proakis, *Digital communications*. New York: McGraw-Hill, 4-th Ed, 2000.
- [33] K. Cho and D. Yoon, "On the general BER expression of one- and two- dimensional amplitude modulations," *IEEE Trans. Commun.*, vol. 50, pp. 1074–1080, Jul. 2002.
- [34] Y. L. Xu, J. Weng, and T. Le-Ngoc, "Adaptive Tone Diversity for OFDMA in Broadband Wireless Communications," *Vehi. Tech. Conf., VTC2004-Spring, Milan, Italy*, May 2004.
- [35] T. Eng, N. Kong, and L. B. Milstein, "Comparison of diversity combining techniques for Rayleigh fading channels," *IEEE Trans. Commun.*, vol. COM-44, pp. 1117–1129, Sept. 1996.

- [36] E. A. Neasmith and N. C. Beaulieu, "New results on selection diversity," *IEEE Trans. Commun.*, vol. COM-46, pp. 695–704, May 1998.
- [37] J. M. Cioffi, "A multicarrier primer," ANSI T1E1.4 Committee Contribution, Amati Communications Corporation and Stanford University, Nov. 1991.
- [38] V. Erceg, K.V.S. Hari, M.S. Smith, *et al.*, "Channel models for fixed wireless applications," in *IEEE 802.16.3c-01/29r4*, IEEE, Jul. 2001.
- [39] C. Suh, C. S. Hwang, and H. Choi, "Comparative study of time-domain and frequency-domain channel estimation in MIMO-OFDM systems," *Personal, Indoor and Mobile Radio Communications, PIMRC 2003, 14th IEEE Proceedings on*, vol. 2, pp. 1095–1099, Sept. 2003.
- [40] A. Leke and J. M. Cioffi, "Impact of imperfect channel knowledge on the performance of multicarrier systems," in *Proc. IEEE Global Telecommun. Conf., Globecom98*, vol. 2, pp. 951–955, Nov. 1998.
- [41] S. Verdu, *Multiuser Detection*. Cambridge University Press, 1998.